Analyzing Tool Dynamics and Surface Roughness Variation for Low Depths of Cut when Milling 6061-T6 Aluminum

Analyzing Tool Dynamics and Surface Roughness Variation for Low Depths of Cut when Milling 6061-T6 Aluminum

PAVEL DAITCH P.Eng.

A Thesis Submitted to the School of Graduate Studies in Partial Fulfilment of the Requirements for the Degree Master of Applied Sciences

McMaster University, Hamilton, Ontario, Canada

MASTER OF APPLIED SCIENCE (2023) McMaster University

(MECHANICAL ENGINEERING) Hamilton, Ontario, Canada

TITLE: Analyzing Tool Dynamics and Surface Roughness Variation for Low Depths of Cut when Milling 6061-T6 Aluminum

AUTHOR: Pavel Daitch P.Eng., Mechanical Engineering

SUPERVISOR: Dr Stephen C. Veldhuis

Department of Mechanical Engineering

McMaster University

NUMBER OF PAGES: xviii, 91

ABSTRACT

This study explores the relationship between endmill tool dynamics and cutting parameters, emphasizing the impact of these factors on machining dynamics, surface finish, and dimensional control. It introduces a novel approach to analyze and optimize the overall performance of a solid carbide endmill, with a specific focus on machining Aluminum 6066-T6. By using stability lobes diagrams (SLD), stable conditions for cutting were chosen, and then surface roughness and tool and workpiece vibration analyses were performed to assess machining performance. This work aims to understand the effects of operating below the peaks and valleys, inherent in the shape of the SLD, using different RPMs. The study's methodology involves tap tests using CutPro - Tap Test Module and milling tests on a horizontal machining center. The surface roughness measurement was performed using an Alicona Infinite Focus confocal microscope and accelerometers were positioned on the spindle bearing housing and workpiece. The findings suggest that within the stable range below the stability lobe diagram's boundary, there is a significant difference in vibration resulting in variation in surface roughness corresponding to the peaks and valleys of the SLD. The variation of acceleration, and consequently vibration, was considerably higher when operating below valleys which negatively affected the surface roughness of the workpiece. The surface roughness plays a pivotal role in tool performance and subsequently influences metal removal rate and tool and spindle life. For conditions

closer to instability, this is even more important. In conclusion, this research lays the foundation for a holistic approach to solid carbide endmill design and cutting parameter selection, showing that the machining process can be optimized in terms of the SLDs, even in regions far below the stability limit.

Keywords: Surface finish, machine tool dynamics, milling, stability, aluminum, cutting parameters, vibrations.

ACKNOWLEDGEMENT

First and foremost, I want to express my heartfelt appreciation to Dr. Stephen Veldhuis, not only for his supervision and support but also for the invaluable learning opportunities and the sharing of his knowledge over the past three years.

Additionally, I extend special thanks to Dr. Jose Mario Paiva for his guidance and friendship throughout the years, Mohammad Shariful Islam Chowdhury for providing support on Alicona measuring equipment, the Machining Systems Laboratory staff, especially Mr. Alam for their significant assistance with the Tap Test procedure, Monica Costa Rodrigues Guimaraes for her help with Minitab analysis, Brady Sample for maintaining an excellent work environment in the lab, and for personal and technical support.

I would also like to express gratitude to all the friends I made at MMRI, my lab mates, and everyone who not only contributed to this work but also provided personal support. Special mention goes to Victor Saciotto and Patrick Chin for their substantial contributions to data generation and analysis using Matlab.

A big thank you goes to Epic Tool for providing flexibility and maintaining a work-life balance during studies and exams.

Lastly, but certainly not least, I want to thank my family for their unwavering support, patience, and consideration.

CONTENTS

NOTATION AND ABBREVIATIONS

SYMBOL	MEANING	UNITS
SLD	Stability Lobe Diagram	
SLDR	Stability Lobe Diagram Random	
SLDP	Stability Lobe Diagram Peak	
SLPV	SLPV - Stability Lobe Diagram Valley	
FRF	Frequency Response Function	
CNC	Computer Numerical Control	
R_a	Average Surface Roughness	µm
F_x	Force in X direction	N
F_y	Force in Y direction	N
F_z	Force in Z direction	N
MRR / Q	Metal Removal Rate	mm^3/min
DAQ	Data Acquisition Card	
V_c	Cutting Speed	m/min
F_z	Feed per Tooth	mm/t
ap	Axial Depth of Cut	mm
ae	Radial Depth of Cut	mm
Ω	Revolutions per minute / Spindle speed	RPM
z	Number of cutting flutes	#
m	Mass	kg
k	Stiffness	N/m
c	Damping	N·s/m
b_{lim}	Limiting axial depth to avoid chatter for a selected spindle speed	mm
K_s	Specific cutting force	N/mm^2
Re[Gorient]	Negative real part-oriented frequency response function	
b	Chip width	mm
N_0	Vibration amplitude in the surface normal direction from the previous cutting pass	mm
N	The current vibration amplitude	mm
f_c	Chatter frequency	(Hz)

J	The number of complete vibration periods between teeth (i.e., the lobe number)	#
h	Theoretical surface roughness	μm
Re	Cutting edge corner radius	mm
h_{ex}	Uncut chip thickness	mm
D_c	Effective cutting tool diameter	mm
ω_n	Natural frequency	Hz

LIST OF FIGURES

LIST OF TABLES

THESIS OUTLINE

This thesis is separated into five chapters as per following:

CHAPTER 1 – INTRODUCTION:

This chapter talks about productivity and machine tool dynamics process parameters selection and describes the research motivation. In addition, the research objectives are presented.

CHAPTER 2 – LITERATURE REVIEW:

This chapter provides detailed overview of the fundamentals of the metal cutting and milling process including machine tool dynamics process parameters characterization. Different endmill designs and machine dynamics parameters affecting process optimization found in contemporary scientific literature are extensively reviewed. The productivity in machining and surface integrity are discussed.

CHAPTER 3 – METHODOLOGY:

This chapter presents detailed information on the experimental setups of the cutting tests, including the experimental methodology.

CHAPTER 4: RESULTS AND DISCUSSION:

The experimental results obtained in this study are presented and assessed in detail. Effect of the RPM on the surface finish in the stable zone of the SLD is discussed.

CHAPTER 5 – CONCLUSIONS & FUTURE WORKS.

This chapter summarizes and highlights the important findings of this research for optimised tool performance that incorporate two parameters: spindle RPM and surface finish output.

CHAPTER 1 – INTRODUCTION

1.1 BACKGROUND

In an era of global competition and rapid technological advancements, industries such as aerospace, automotive, and die and mold manufacturing face a pressing need to enhance productivity while simultaneously reducing costs and upholding or even improving product quality. An essential component of productivity improvement is the enhancement of the metal removal rate (MRR). However, this pursuit of increased MRR can lead to stability issues during machining, often manifesting as the dreaded phenomenon of chatter. Chatter, as shown in Figure 1, is a disruptive condition in machining, contributing to adverse effects such as poor surface finish, diminished dimensional accuracy, longer cycle times, reduced tool lifespan, and potential damage to machinery equipment. The implications of poor surface finish are not limited to aesthetics but extend to the ultimate performance and functionality of the manufactured parts. Additionally, the increased cycle time and shortened tool life significantly elevate production costs.

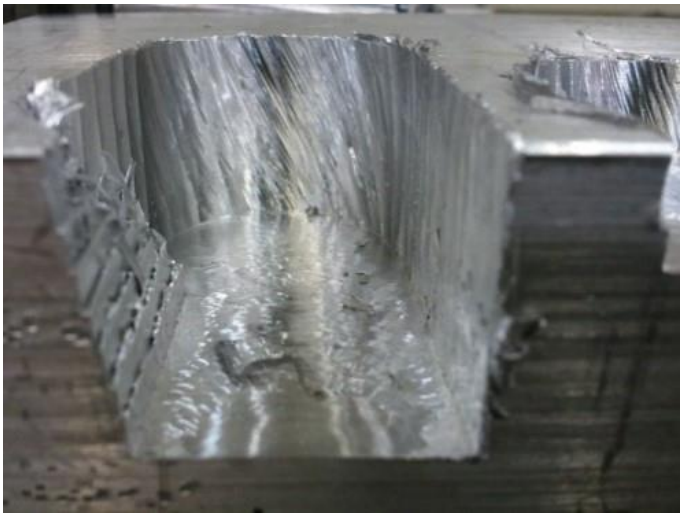

Figure 1: Sample of a chatter marks.

Given these challenges, it becomes imperative to address chatter at the earliest stages of the process design. Effective chatter control encompasses a range of techniques, including but not limited to specialized tool design, meticulous selection, and optimization of cutting parameters, strategic machining approaches, increased structural stiffness, and improved dampening mechanisms. However, what sets this thesis apart is its holistic approach to cutting process design, focusing on milling process performance and the optimization in conjunction with cutting parameters.

The proposed methodology in this thesis aims to introduce a novel perspective on the integration of tool dynamics and cutting speed, offering a comprehensive solution to surface finish enhancement. This innovative approach is assisted by the use of resonance matching charts to guide experimental design, allowing a deeper understanding of the relationship between specific cutting

speeds and surface finish quality. To further illustrate these concepts, this research will include images of machining processes, highlighting the convergence of tool dynamic elements, and cutting parameters (specially cutting speed) and their impact on vibration levels and surface finish.

In essence, this thesis presents a method to address the fundamental challenges of productivity, MRR enhancement, and chatter control in manufacturing industries. Through the development of a holistic approach that combines tool dynamics with optimized cutting parameters, it seeks to provide a unique and valuable contribution to the field of metalworking, ensuring that the search for increased productivity does not compromise the quality and efficiency of the production process.

1.2 RESEARCH GAPS AND MOTIVATION

1. Current research lacks a holistic approach that combines multiple machining parameters like surface finish with the selection of machine tool dynamics parameters like tool design and cutting speed.

2. Information is scarce regarding the collaborative role of multiple parameters in achieving high performance operations.

3. There is a noticeable absence of data concerning surface roughness below the b_{lim} of the Stability Lobe Diagram (SLD) and its subsequent impact on the dynamic machining process [[1], [2], [3]].

Based on the previous statements found from the literature review, the core motivation behind this research is to reduce vibration and to have better understanding of the surface roughness generated for low depths of cut well within the stable zone of SLD. Ultimately, the goal is to increase cutting speed to enhance productivity while meeting quality targets and simultaneously prolonging tool and machine lifespan which impacts cost. This achievement holds the key to significant cost benefits in high volume production environments. A powerful visual representation, capturing this notion, is crucial to convey the essence of productivity gains as per SLD Figure 2.

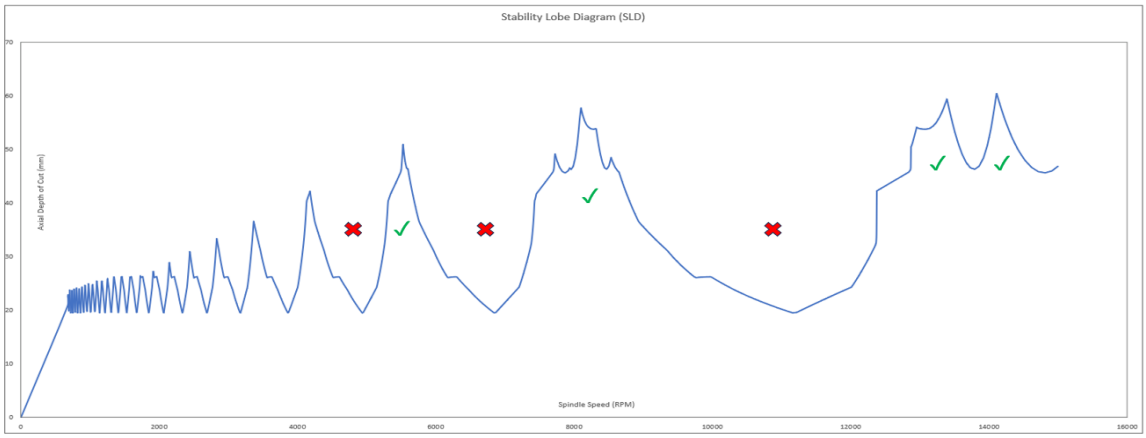

Figure 2: Stability Lobe Diagram (SLD)

1.3 RESEARCH OBJECTIVES

The aim of this research is to achieve the ideal combination of machining tool design and process parameters specifically tailored to a given workpiece material. This research strives to establish a holistic approach to optimizing cutting tool designs by seamlessly integrating them with the most suitable cutting parameters.

In this work, the investigation is focused on evaluating the performance of solid carbide endmills within the stable region below the b_{lim} of the Stability Lobe Diagram (SLD) during slotting operations, maintaining a consistent cutting axial depth and feed rate. The selection of RPM from the SLD forms an integral part of the study.

The research goals can be summarized as follows:

1. Investigate the impact of milling 6061-T6 Aluminum below the b_{lim} of SLD on surface roughness values, aiming to understand its influence on the process and enhancing productivity.
2. Establish a systematic guide and analytical framework for the selection of optimized process parameters in the machining process, contributing to a more efficient and effective manufacturing approach.
3. Fine-tune cutting tool designs based on the identified process requirements, ensuring optimal alignment for enhanced performance and productivity.

CHAPTER 2 – LITERATURE REVIEW

2.1 FUNDAMENTALS OF THE METAL CUTTING

Trent [4] in his book described the metal cutting or machining process the operations in which a thin layer of metal, the chip or swarf, is removed by a wedge-shaped tool from a larger body to shape a material to a desired dimension and surface finish. It can be referred not just to metals, but wood, plastic, and other materials. Machining is one of the most popular ways to make parts for many different industries thus machining plays big role in the global economy realizing billions of dollars in produced parts per year.

The machining process involves the cutting edge moving relative to the workpiece, resulting in the shearing of material layers. Machining process is one of the most complicated subjects in mechanical engineering and is driven by process parameters such as workpiece and cutting tool material, cutting speed, feed, depth of cut, tool geometry, cooling technique etc. Even minor changes in parameters may lead to process output variation. For example, surface integrity, cutting forces, pressure, and temperature.

2.1.1 Metal cutting in general

Regardless of what metalworking process we are talking about, the cutting principle is based on the relative motion between the cutting edge of the tool [5] and the workpiece due to the high strain rates, temperature, and forces generated in the cutting zone.

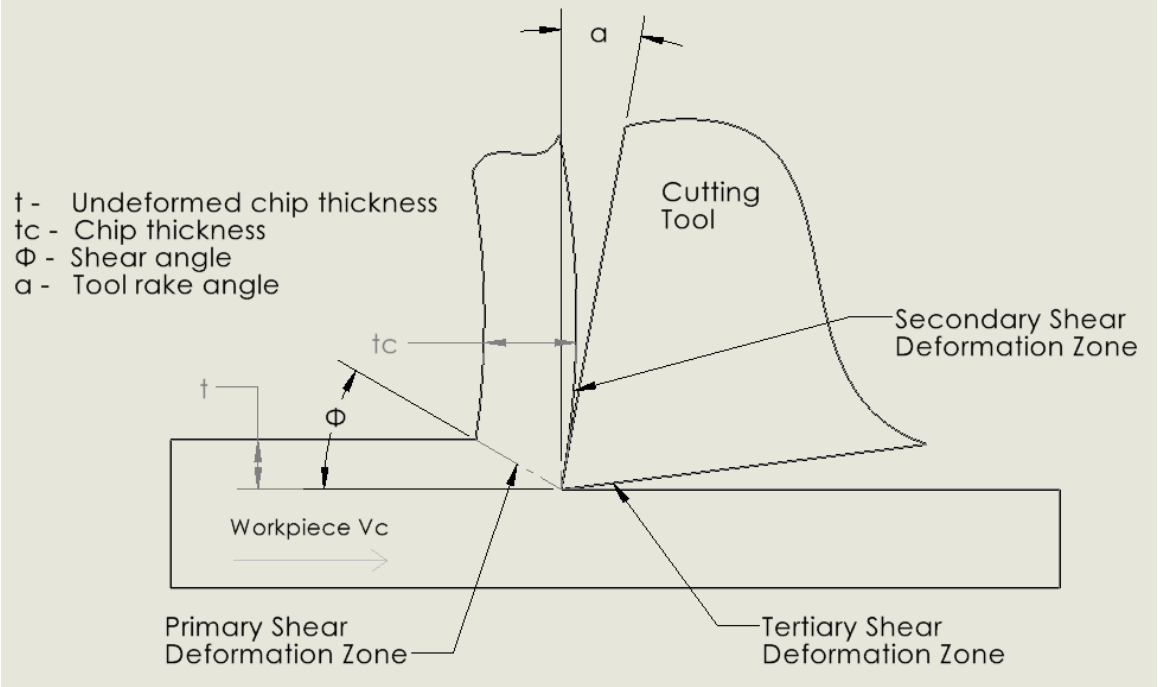

Figure 3: Cutting deformation zones schematics based on [1].

Figure 3 illustrates three significant regions in the cutting process, signifying three shear zones where the primary phenomena governing the process occur. The primary deformation zone is where plastic deformation takes place during metal cutting. Material is directed towards the cutting edge, experiencing intense

plastic deformation on the shear plane, thereby requiring a considerable amount of energy [2].

In the secondary shear deformation zone, the cutting chips slides over the top rake face of the cutting tool, causing friction. The chip, plastically deformed with a thickness represented by tc (where tc is greater than t), glides along the top rake face at an orientation denoted as "α," leading to the generation of exceptionally high stresses.

The creation of the Tertiary Shear Deformation Zone is a result of the friction between the primary clearance face of the cutting tool and the workpiece material. This friction leads to tool wear, impacting the surface integrity of the part surface [2].

2.1.2 Cutting temperature

Cutting temperatures affect machining performance [2]. The temperature is directly affected by machining process parameters and workpiece material. Increasing the cutting speed, feed, and depth of cut raise the cutting temperature. The influence of cutting speed on cutting temperature has the highest impact. Out of the three parameters, the depth of cut has the lowest impact on the temperature in the cutting zone.

2.1.3 Cutting forces

Cutting forces stand out as crucial parameters in the machining cutting process. They not only determine the power consumed during cutting but also influence various aspects of the environment, encompassing cutting parameters, machine stability requirements, cutting fixture design, coolants, and more.

Understanding, modelling, and assessing machining operations depend on the cutting force signal. It can be used for process improvements, chatter detection, tool wear evaluation and the tool breakage detection. For measuring cutting force, the dynamometers are a common option [5]. The multi-axis piezoelectric sensor been used.

Typically, cutting forces decrease as cutting speed increases [4]. The main considerations restricting the size of the cutting-edge corner radius are deflection and chatter because the increase in the corner radius leads to higher radial cutting forces.

2.1.4 Machinability of Aluminum Alloys

The machinability of a metal is defined by how easy it’s to machine, which is difficult to quantify and is used more as a relative qualitative property [4][1]. Aspects of machinability that are commonly encountered are power, cutting temperature, power density, tool life, surface roughness or polish, and tooling cost.

In general, the harder a material is to machine, the higher the shear stress or particular power values. Machinability is measured relative to the results achieved on Steel SAE 1112 at a hardness of 160 Brinell.

Among the major metals, aluminium alloys are among the easiest to machine. Aluminum alloys [2] been extensively used in Aerospace and Automotive industries for its relatively high strength to weight ratio [6].

The machinability of aluminium material is compared both within its own types and with other metals in Figure 4.

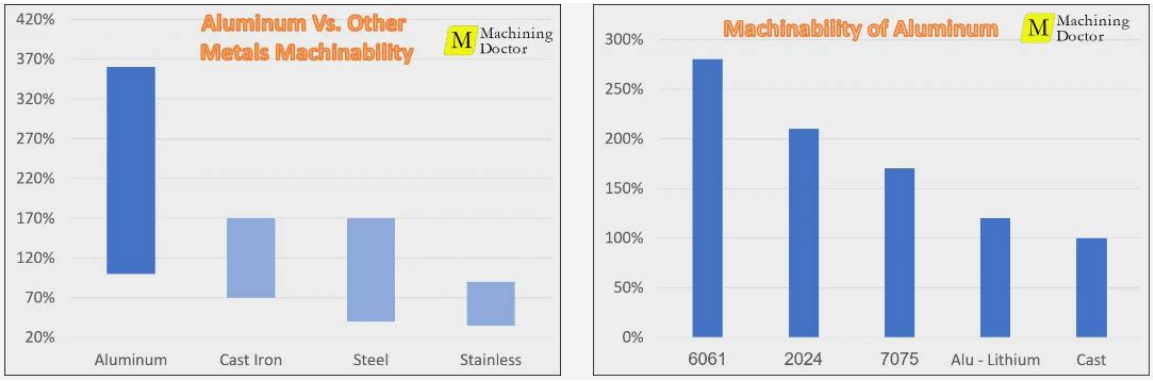

Figure 4: Left-Aluminum vs other metals machinability; Right-Machinability of aluminum. Used with permission [7].

The 6061 alloy stands out as the most widely used alloy within the 6XXX aluminum series, renowned for its versatility across various engineering applications. In particular, 6061-T6 (Unified Numbering System designation A96061) denotes an aluminium alloy that has been precipitation-hardened, with silicon and magnesium acting as its main alloying constituents relative to other alloys. The T6 designation signifies its precipitation-hardening heat treatment, a

method established in 1935. Aluminum 6061-T6 material is characterized by favorable machinability and mechanical properties, as well as commendable weldability and extrudability. Furthermore, its versatility in coating applications—like anodizing and Alodine coating—allows for improved resistance to corrosion and wear. While possessing an average fatigue strength, it's worth noting that the temper T6 process in 6061 aluminum exhibits limited formability compared to the T4 temper process. Additionally, its extrudability makes 6061 a preferred material [8].

2.2 MILLING PROCESS

2.2.1 General aspect of milling operation

Machining is the manufacturing process of shaping metal by removing undesirable material from it. This process can be performed in different ways including cutting, turning, drilling, milling, grinding, broaching, etc.

In milling operations, a rotating cutter is utilized to remove material from the workpiece [2]. As per Figure 5, milling operations encompass a variety of techniques like, slotting, face and shoulder milling, profiling etc.

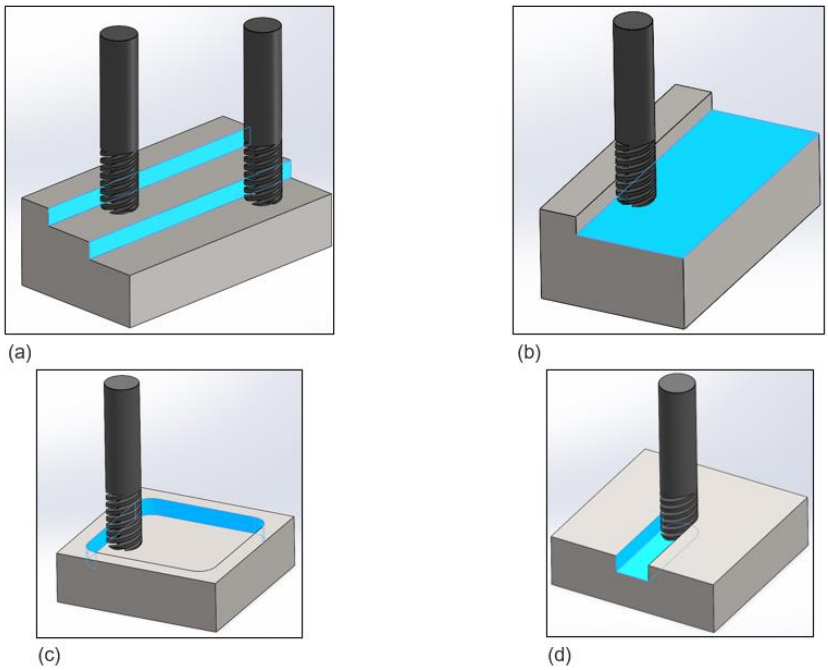

Figure 5: Types of milling operations: (a) shoulder milling, (b) face milling, (c) profile milling, (d) slot milling.

2.2.2 Down (or climb) vs Up (or conventional) milling

Milling processes are divided into down (or climb) and up (or conventional) milling operations (Figure 6) [9]).

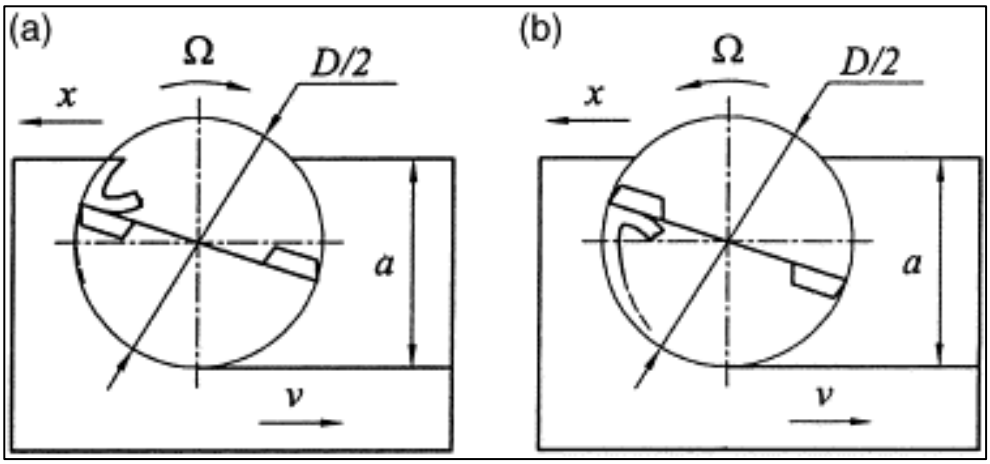

Figure 6: (a) Up (or conventional) and (b) Down (or climb) milling [9].

When down milling, or climb milling, is used, the cutting tool advances in the direction that it rotates. When conditions of the machine tool, fixture, and workpiece allow, down milling is always the preferred method.

In peripheral down milling, the chip thickness gradually approaches zero at the end of the cut, starting to decrease from the beginning. This keeps the tool edge from burnishing or rubbing against the surface before the cutting action starts. On the other hand, the cutting tool's feed direction is the opposite of its rotation during up milling, also known as conventional milling. As the incision deepens, the chip thickness starts at zero and increases. In this case, the cutting edge must be

forced into the cut, which causes a rubbing or burnishing effect because of friction, high temperatures, and oftentimes, contact with a surface that has been work-hardened by the previous edge. All these elements work together to shorten the tool life.

Both, down (or climb) and up (or conventional) milling have advantages and disadvantages depends on the applications.

When there is backlash in the spindle and feed drive, or when the item has significant height changes, or when it has an exterior layer that has been hardened via sand casting or flame cutting, up-milling is usually preferred to down-milling. The possibility of a chip becoming lodged between the insert and the cutter during down-milling increases the chance of tool breakage. However, peripheral down-milling helps to fix the item on the machine and reduce cutting vibrations if the spindle and drive are stiff. When it comes to machining nickel alloys and other materials that are vulnerable to surface damage, down-milling is the method of choice. This is so that the possibility of burnishing is reduced during down-milling because the tool's margin and flank do not come into contact with the machined surface. [2].

Throughout the milling process, the uncut chip thickness varies continuously, as seen in Figure 7. When up-milling, the chip thickness is initially tiny at the beginning of the cut and progressively grows as the cutting progresses. On the other hand, while down-milling, the chip thickness is greatest towards the beginning of the cut.

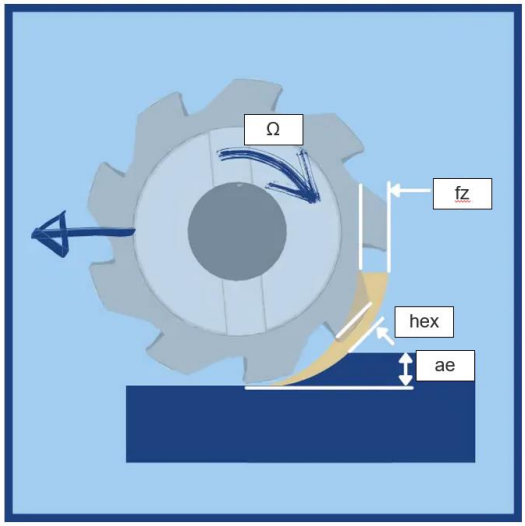

Figure 7: Uncut chip thickness (hex). (Adopted and used with permission [7])

The uncut chip thickness (hex) is subject to variation based on factors such as cutter diameter and working engagement, specifically the radial immersion of a cutter denoted as ae/Dc. If this value is less than 50%, there is a reduction in the maximum chip thickness compared to Fz.

2.3 CUTTING TOOLS

Cutting-tool geometry has an impact on cutting parameters and machining performance. Choosing the right cutting tool is crucial for ensuring a successful cutting operation. This is because the tool's shape, form, material substrate, and coating must be well-matched with the type of operation, workpiece material, and cutting conditions [1]. During the machining process, cutting tools experience high compressive stresses and temperatures spikes, and as a result, need to be

chemically and thermically stable, hard, yet tough to manage interrupted cuts and provide fatigue resistance to repeated loading [2].

2.3.1 Tool geometry

Tool geometry significantly affect different aspects of the machining process that include but are not limited to:

- Uncut chip or actual chip thickness – The optimal uncut chip thickness is required to achieve the maximum productivity and avoid tool rubbing.
- Chip control - Affects the chip thickness, the chips flow direction.
- Tool Life: Affects tool life by altering magnitude and direction of forces, friction and temperature distribution.
- Forces: Affects the direction and magnitude of forces.
- Quality: Affects the surface integrity.

2.3.1.1. Solid Carbide endmill design

Numerous studies have researched endmill design and dynamics, with a focus on selecting cutting tool parameters on a tool and workpiece basis. However, many of these investigations have not sufficiently considered the interaction between these parameters in the context of tool dynamics and the preferred cutting

parameters that significantly impact overall process performance. Furthermore, certain studies have explored the influence of grinding wheel spindle vibration on surface roughness and subsurface damage in the realm of grinding brittle materials like carbides used for cutting tools [10].

Additionally, there has been a proposal for an innovative chatter-free milling strategy, involving an end mill with a large number of flutes and a high-speed, high-power machine tool, to enhance milling efficiency and precision [11].

To further the understanding of the milling process, a simple milling model has been adopted to calculate the forces involved, providing a foundational framework for analysis and optimization [12].

2.3.1.2. **Variable pitch endmills**

Slavicek studied the effect on uneven pitch cutters and showed that the optimal pitch depends on the chatter frequency, if the target is to improve the stability under certain cutting speed [13]. Also, this study revealed that one can't improve the stability under all cutting speeds with one specific selected tooth pitch design configuration.

Shirase et al. show that an irregular tooth pitch end mill can lead to an increase of stability and reduce surface error [14]. Suzuki et al., realised the importance and proposed a new design method of irregular pitch end mills to

achieve high productivity in milling [15] and Hayasaka et al., proposed a design method of irregular pitch end mills to achieve high productivity in milling [16].

2.3.1.3. **Tools with non-uniform geometries**

Serrated tools, originally proposed by Strasman, have garnered attention in research endeavors. Tehranizadeh conducted an insightful investigation into the mechanics and dynamics of milling with crest-cut end mills. This study revealed that crest-cut end mills exhibit broader and higher stability lobes compared to standard milling tools. This enhanced stability is attributed to non-periodic cutting forces generated by the wave edge geometry [17].

In a distinct study, Junz Wang and Yang explored the modeling of angle and frequency domain forces for a roughing end mill featuring a sinusoidal edge profile [18]. Their findings underscored the influential roles played by the wave amplitude and pitch in shaping the chip load kinematics of the roughing end mill. Their research demonstrated that, for an N-flute roughing end mill with a feed ratio surpassing a certain undulation amplitude to the feed per tooth ratio, only the crest portion of the cutting edge engages in the cutting process. This results in a chip width equal to 1/Nth of the pitch of the sinusoidal wave edge. Importantly, this reduction in effective axial depth of cut proves pivotal in enhancing machining stability and allows for a higher apparent axial depth of cut for a roughing cutter.

Moreover, Bari et al. employed graphical-frequency domain methods to analyze serrated end mills [19]. Their research highlighted substantial benefits derived from the non-uniform geometry, particularly when machining difficult-to-cut materials. The serrated end mills exhibited superior stability characteristics and heightened productivity due to the irregular distribution of chip thickness and varying time delays along their flutes. These characteristics disrupt the regenerative chatter mechanism and thereby maximize productivity in rough machining operations.

2.3.1.4. **Variable helix endmills**

Further research was done on several kinds of special end mills, like variable helix, as a result of studies demonstrating the benefits of special end mills.

Imad in his work has investigated the importance of edge preparation on the milling tool and found that different edge radii didn’t show a measurable difference in the surface roughness. Also, when you increase the edge radii, the feed marks become more visible and depth of cold working and microhardness increases [20].

2.3.2 Tool materials

Various cutting tool materials find application in machining processes, each tailored to specific demands. These consist of single-crystal diamonds, polycrystalline cubic boron nitride (PCBN), Cermet, carbon steels, high-speed steels (HSS), tungsten carbide, and ceramic materials. The selection of cutting tool materials is crucial, as these materials must withstand the high stresses and temperatures generated during the cutting process and chip formation.

Key properties of cutting tools include high hardness and Elastic modulus, essential for reducing abrasive wear and edge deformation, particularly in turning operations. Moreover, high fracture toughness is imperative to counteract tool breakage, especially in milling operations characterized by interrupted cuts. Chemical inertness is a desirable trait, particularly when cutting aluminum, to resist diffusion and chemical wear.

Some cutting tools are designed with high thermal conductivity characteristics, such as PCD, to effectively reduce cutting temperatures in the cutting zone. Additionally, high fatigue and thermal shock resistance are essential features, particularly in end-milling roughing operations where interrupted cuts are prevalent. Sustaining high stiffness is crucial to improve process dynamics and ensure precision in machined parts.

Furthermore, cutting tool materials often possess lubricity features, helping to minimize friction and prevent Built-Up Edge (BUE), especially when working with

sticky or ductile materials. The complex balance of these material properties ensures optimal performance and durability across a diverse range of machining applications.

The link between different tool materials and toughness on a horizontal axis and hardness on a vertical axis is depicted in Figure 8 [21]. The Increase in the hardness is typically accompanied by decrease in the toughness and vice versa.

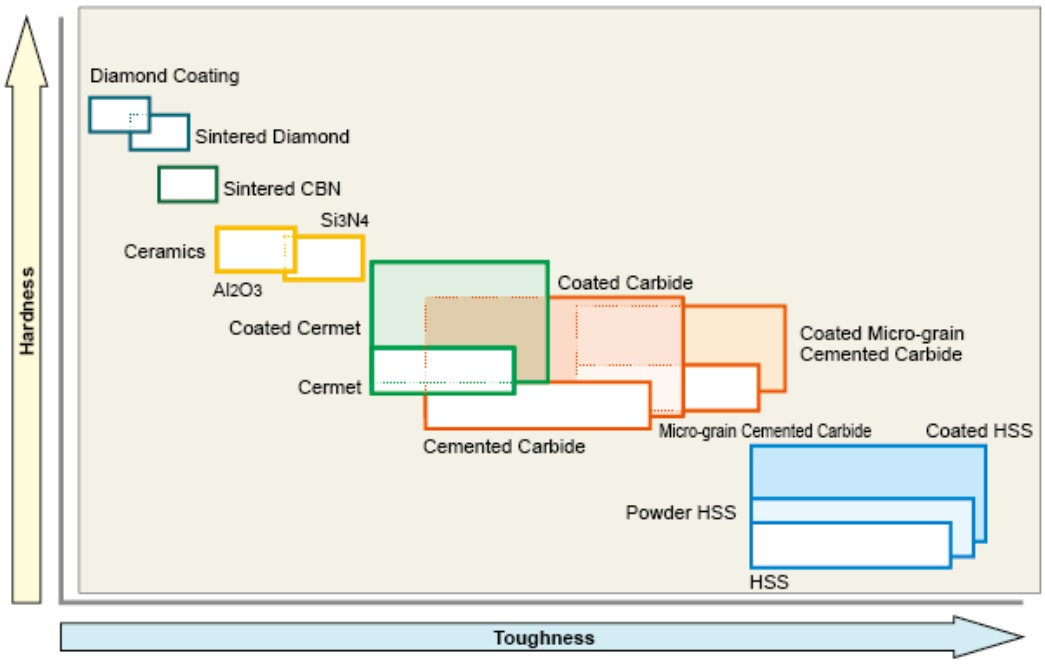

Figure 8: Cutting tool materials Hardness VS Toughness [21].

2.3.3 Tool wear

Tool wear is inevitable in machining cutting process were cutting tools experience various forms of gradual or progressive tool wear. The wear mechanism and modes depend on workpiece with cutting tool material and cutting parameters and conditions (especially the cutting speed) also playing an important role. Tools can also fail due to premature breakage and fracture due to excessive loads of fatigue.

D. A. Stephenson and J. S. Agapiou [2] delineate five distinct wear mechanisms: adhesion, abrasion, diffusion, oxidation, and chemical wear.

- Adhesive wear is identified by the adherence or welding of chips to the tool surface caused by friction and sometimes an affinity between workpiece and tool materials. Small particles of the tool weld to the chips and carried away. High adhesive wear may lead to build-up-edge (BUE) and result in tool catastrophic breakage.
- Hard particles scrape and remove material from the tool, including substrate and coating, causing abrasive wear.
- Diffusion wear takes place when heightened temperature and contact lead to the diffusion of the tool material components into the chip.
- Oxidation refers to the chemical reaction between tool components, primarily the binder, and atmospheric oxygen.

- Chemical wear arises from chemical reactions occurring between the tool and the workpiece on the flank and rake faces.

In addition to the wear mechanisms described above, there are several other wear types associated with thermal and mechanical effects. Figure 9 [22] shows major wear mechanisms such as cracks and plastic deformation that are dominant in turning.

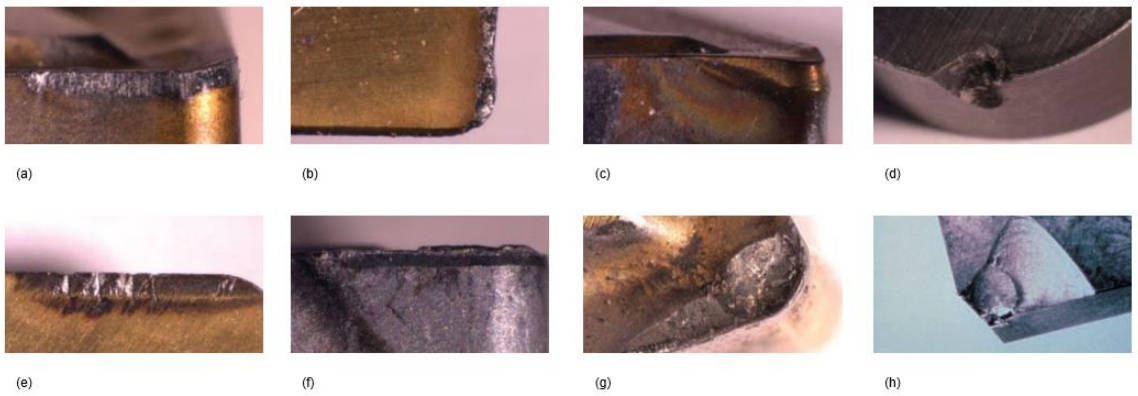

Figure 9 [22]: Tool wear types on indexable cutting inserts : (a) flank wear; (b) edge chipping; (c) plastic deformation; (d) depth of cut notch; (e) thermal cracks; (f) built-up edge; (g) crater wear; (h) catastrophic breakage.

Four primary types of tool wear prevail in carbide end milling, as illustrated in Figure 10 [23]. Abrasive Wear, Chipping, Thermal Cracking, and Fracture.

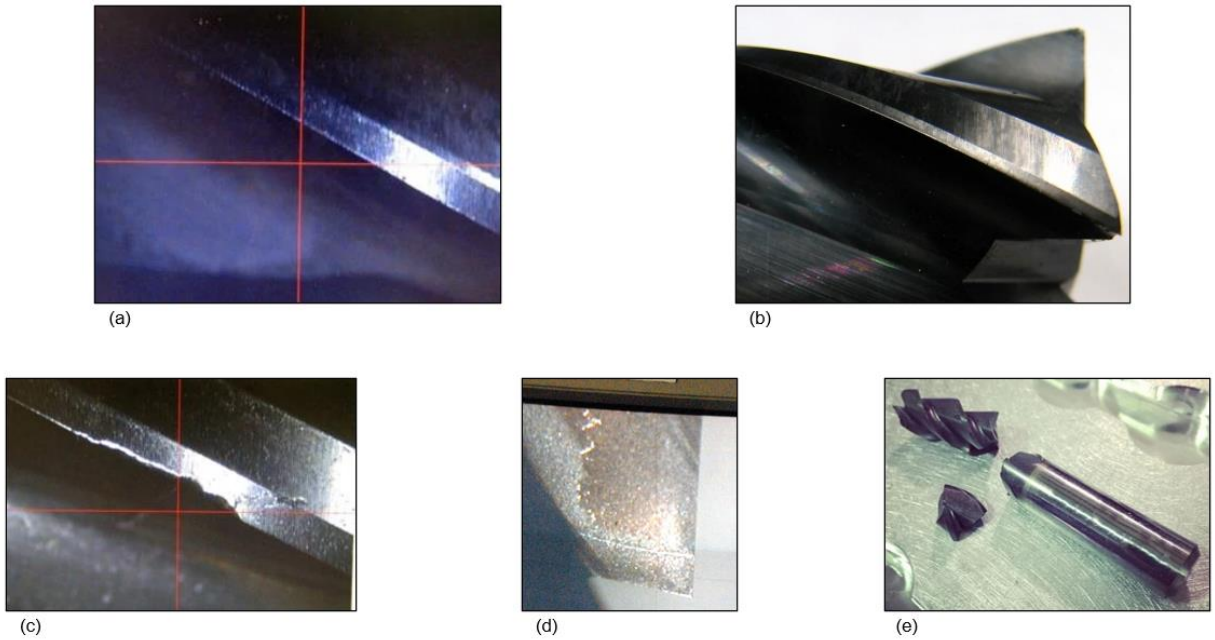

Figure 10 [23]: Dominant tool wear types on milling endmills [22]: (a) Tool with no wear, (b) abrasive wear, (c) chipping, (d) thermal cracking, (e) fracture.

2.4 PRODUCTIVITY IN MACHINING

Discussing productivity in terms of metal removal rate, which measures the volume of material removed per unit of time during milling operations. The metal removal rate is expressed using an Equation (1), where Q = Metal Removal Rate measured in mm3/min, Fz = chip load (mm/t), z = number of cutting flutes, Ω = Spindle speed in revolutions per minute, ap = axial depth of cut (mm) and ae = radial depth of cut (mm)

$$MMR = Q = F_z \; x \; z \; x \; \Omega \; x \; ap \; x \; ae \text{ [24]} \qquad (1)$$

Based on the insights of previous studies [25], the research investigates the relationship between heightened productivity and enhanced quality, emphasizing the pivotal role of elevating surface roughness as a strategic avenue for optimizing productivity in the machining process.

2.4.1 Parameters that effect productivity

The quality of surface finish and rate of metal removal are largely dependent on the dynamics of the machine tool and the choice of suitable machining parameters [26].

For milling processes to be optimised, a number of critical cutting conditions are essential. These conditions include cutting force, feed rate, depth of cut, cutting

speed, spindle speed, width of cut, and feed per tooth [27]. In a study aimed at optimizing P20 milling operations, it was determined by Daniyan [24] that the optimal performance of the cutting tool is complexly linked to certain critical parameters. Among these, the feed rate and cutting speed stand out as they have a significant impact on the rate of material removal and the resulting surface finish.

In order to optimize the milling operation for aluminum alloy (AA6063 T6), a rigorous process design and optimization were conducted, employing the Response Surface Methodology [24]. Through meticulous statistical and physical analyses, it was elucidated that the optimization of parameters related to actual cutting energy and power consumption during the cutting operation holds the potential to significantly enhance the overall sustainability of the manufacturing process. This optimization extends to the reduction of carbon footprint, improved energy efficiency, and heightened environmental friendliness of the machining process.

In a parallel study focused on the optimization of Milling Aluminum Alloy 6061-T6, Suyang [28] found the presence of a critical cutting speed in the cutting process of AA 6061-T6. Notably, surpassing this critical speed resulted in a simultaneous decrease in both cutting force and cutting temperature indicating that more heat is being generated which softens the material, but the heat is leaving the cutting zone with the chip.

Further insights into end-milling productivity were gained through Savilov's exploration of the axial contact points method [29]. The study revealed that an

increase in feed per tooth led to a decrease in the tangential component of the cutting force, consequently enhancing productivity within a specific machining system constrained by torque and spindle power limitations. Contrarily, the radial component of the cutting force exhibited an increase with the augmentation of feed per tooth.

2.5 SURFACE INTEGRITY

When designers select the material for their engineering components, they are driven by the natural environment where the specific components will function and how they will operate. The ultimate part performance is a result of the material surface characteristics, exposed area, and environmental conditions [30].

Surface integrity is a function of the machined surface natural condition, including its topographical, mechanical, chemical, and metallurgical state and its relationship to functional performance [30]. For example, a surface generated by drilling will be different from the surface that was generated by reaming and requirements from mechanical component will be different whether it will function under different operating conditions. Surface integrity concerns not just its roughness aspect for example, but also mechanical, physical, metallurgical, and biological. Some of the surface defects include, but not limited to plastic deformation and BUE, feed rate marks, waviness, rubbing marks, material tears, burrs, micro and macrocracks, work hardening and residual stress.

In addition to tool life considerations, machining aluminum poses challenges related to chip and burr control, along with the imperative of achieving optimal surface finish and integrity [6]. Previous work in the machining domain has addressed the influence of process dynamics on surface roughness. In this work, the measurement of surface roughness was conducted using an Alicona Infinite Focus confocal microscope [31]. During variable-parameter processing of freeform

surface components, one notable contribution to the field is the invention of a method for forecasting surface roughness at arbitrary places throughout the entire surface [32].

Research dedicated to the machining of thin-walled parts centers on predicting and controlling milling deformation, implementing deformation compensation strategies, and incorporating process monitoring techniques. In investigating the effect of vibration on surface roughness in aluminium 6061-T6 face milling using sound chatter, Abebe [33] found that low sound amplitude is associated with short waves and low vibration, leading to an enhanced surface finish with high frequency vibration content. This finding contributes valuable insights into optimizing surface quality during machining operations.

Table 1 shows the typical surface finish for basic machining operations.

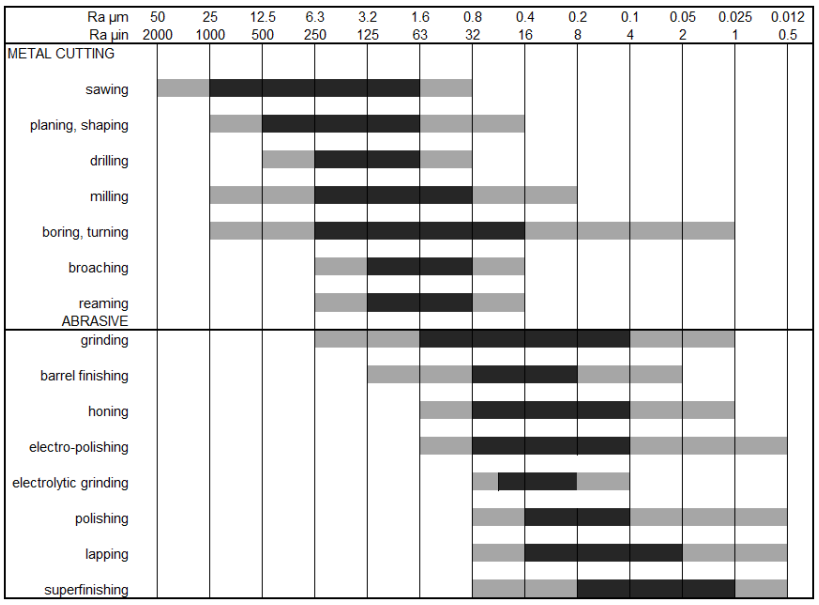

Table 1: Typical surface finish for basic machining operations. Adopted from [34].

Table 2 shows the geometric deviations of machined surfaces according to DIN 4760.

Order	Deviations	Causes
1st	Form errors (flatness, roundness, straightness, cylindricity, etc.)	Errors of machine tool slides, elastic deformations, erroneous fixation of tool or workpiece, severe tool wear
2nd	Waviness	Eccentric rotation of workpiece or tool, vibrations in the manufacturing system (process-tool–workpiece–machine-tool environment), tool wear, inhomogeneity of processed material
3rd	Grooves	Tool edge form, process kinematics, chip morphology
4th	Cracks	Tool-nose wear, built-up-edge formation, mode of chip formation, galvanic procedures
5th	Crystalline structure	Crystallization mode, irregularities due to chemical reactions, corrosive damage
6th	Crystalline formation	Physical and chemical alterations in the material fine structure, deformations of lattice

Table 2: Geometric deviations of machined surfaces (DIN 4760) [30]

The surface topography and texture of the machined area is cutting tool dependant along with cutting parameters and dynamic properties of the entire system that consists of cutting tool, machine holder, spindle, fixture, and the workpiece. For example, the endmill with higher total run-out will produce surface roughness higher than the tool with less total run-out and the cutting insert with wiper design will produce a better surface finish on a lathe.

To characterize the surface quality two terms interchangeably are commonly used – surface finish and surface roughness.

2.5.1 Surface Roughness

The arithmetic average roughness, Ra, is a widely used parameter for assessing surface integrity. It serves as a surface specification for manufactured parts. Ra is calculated as the arithmetic average of deviations (peaks and valleys) around a profile centerline within a specified length, as depicted in Figure 11. Higher Ra values indicate a rougher surface.

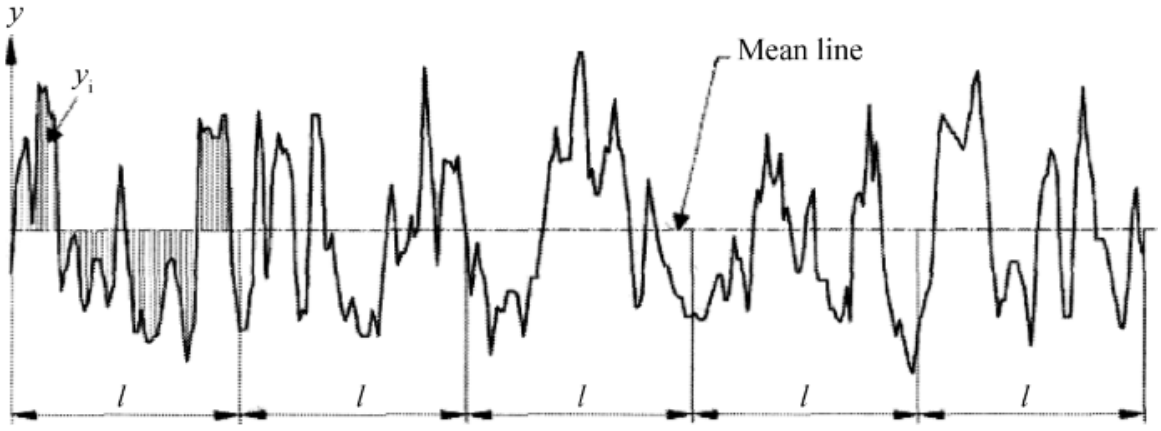

Figure 11: Figure Mean line system and definition of Ra [30]

The theoretical surface roughness h is calculated using the Equation (2), where Fz is the feed per tooth and R_e is the cutting edge corner radius.

$$h = 1000\frac{Fz^2}{8Re} \quad (2)$$

Surface roughness is objectively measured with calibrated equipment, while the Surface finish is used to describe the appearance of the surface for example.

Surface waviness is also a very important machinability parameter that is considered as a symptom of malfunctions in the machine tool system or poor machining, this is a machining dependent variable [30].

2.6 MACHINE TOOL DYNAMICS

Machine dynamics refer to the study of a system's motion based on the forces acting on the system. Chatter is one of the major problems that effect metal removal rate. The regenerative effect was reported as the main reason for chatter [26]. Chatter is a self-excited vibration, depends on many factors, including cutting parameters, dynamic stiffness of the tool-holder-spindle and machine structure system, fixture, workpiece, and tool design characteristics.

A milling cutter with z teeth is considered to have flexibility in two orthogonal directions (x,y) as shown in Figure 12 [35]. The angular position of the cutter changes with time and angular velocity that causes actual chip thickness to change. The relationship between successive cutting-edge passes can generate the conditions for chatter.

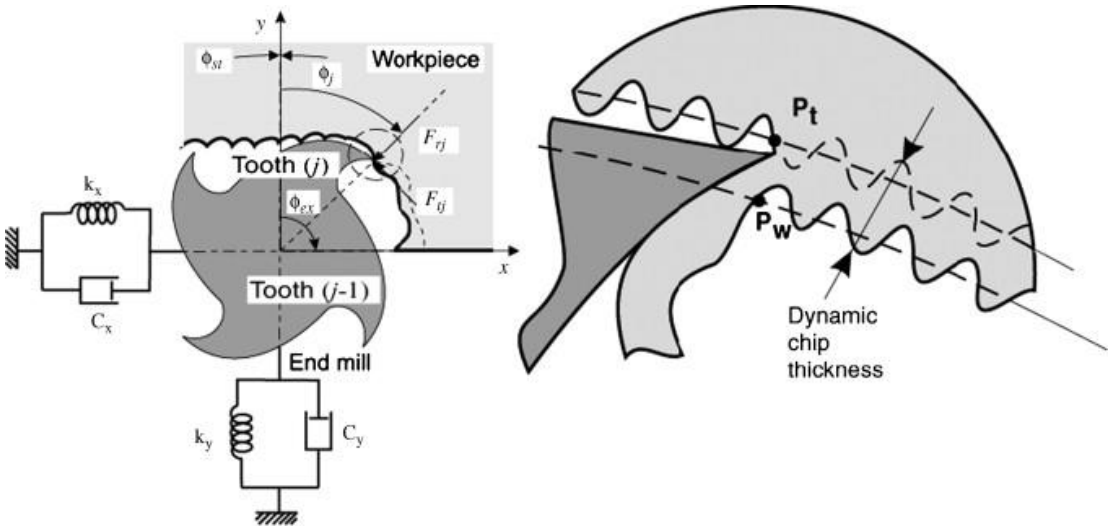

Figure 12: Dynamic milling system [30].

The variable component of the instantaneous cutting force may be written as per Equation (3) [36] where Ks is the specific cutting force, b is the chip width, N_0 is the vibration amplitude in the surface normal direction from the previous cutting pass and N is the current vibration amplitude.

$$F = K_s b(N_0 - N) \quad (3)$$

For the chosen spindle speeds, traditional stability analysis determines the maximum chatter-free axial depth of cut [37]. The limiting axial depth of cut, b_{lim} expression for milling is provided in Equation (4), where z is the number of teeth engaged in the cut, Ks is the specific cutting force, and Re[Gorient] is the negative real part oriented frequency response function that depends on the directional orientation factors and the frequency responses in the x and y directions.

$$b_{lim} = \frac{-1}{2KsRe[Gorient]z} \quad (4)$$

The chatter frequency is expressed in Equation (5), where Ω is the spindle speed, z is the number of teeth on the cutter and J is the total number of vibration cycles (also known as the lobe number) between teeth.

$$fc = \Omega zJ \quad (5)$$

2.6.1 General aspects of machine tool dynamics

Vibrations are broadly categorized into three main types [38]:

- Free Vibration: This occurs when a system, following an initial disturbance, vibrates independently without any external force being applied.
- Forced Vibration: In this case, the system, post-initial disturbance, is subject to an external repeating force.
- Self-excited or Chatter: This involves a harmonic imbalance between the cutting tool and the workpiece and represents a condition where energy builds up in the system as vibrational motion [39].

A comprehensive review on methods for acquiring dynamical property parameters in machining processes is presented [40]. The research highlights that using suitable methods to derive dynamical parameters improves the prediction accuracy of Stability Lobes Diagram, which are essential for creating efficient chatter-suppression mechanisms in a range of machining processes. It highlights the importance of understanding the dynamics of a machine and tool using a tap test process.

Additionally, other works have introduced a neural network-supported inverse parameter identification approach for stability predictions in milling [41]. The approach demonstrated its applicability in identifying both static parameters, which remain constant under operational conditions, and parameters dependent

on one or more influencing factors. This advancement contributes to a deeper understanding of the dynamic behaviour of milling processes, facilitating improved stability predictions.

2.6.2 Cutting forces

Understanding the forces acting in milling is of fundamental importance for the dimensioning of the system, as well as for the capability to obtain narrow tolerances. However, dynamic modelling of the milling process is challenging, due to the cyclical variation in chip thickness, leading to fluctuations in cutting forces. Moreover, the interrupted cut results in impacts between the tool and workpiece, consequently escalating vibrations, further complicating the analysis [12].

Chatter vibrations are a significant obstacle to productivity in machining operations, resulting in poor surface quality, shortened tool lifespan, and potential damage to mechanical components throughout the system [42]–[44].

Stability lobes diagrams (SLD) establish a relationship between the tool's rotational speed and the chatter free axial depth of cut (ap) [45]. Their purpose is to identify the range of machining parameters that yield the highest material removal rate without chatter. The boundary between stable and unstable cutting conditions is determined by the spindle speed and depth of cut [46].

Understanding the effect of cutting forces in dynamics of milling processes is important because its time-dependant nature that excites the structural dynamics

of the tool-holder-spindle-machine-fixture and workpiece. This affects the stability, accuracy, and surface finish of the workpiece.

There are 3 main force components that effect the chatter.

- Cutting Force that is causing forced vibration.
- Dynamic Force related to regenerative effect. Includes depth of cut and the regenerative delay.
- Process damping force. Which can be improved by using cutter special edge geometries.

2.6.3 Tap test

It is crucial to consider machining dynamics when selecting cutting parameters. This leverages new technology advancements to increase productivity and efficiency of current machine tools.

The construction of the SLD is usually done through the system frequency response function (FRF) and force coefficients. The efficiency of the model depends on the correct determination of these coefficients, which are usually obtained through experimental tests [47]. The dynamic response of the system must also be known, which can be measured by its Frequency Response Function (FRF), generally obtained by an impact test at the tip of the cutter.

You can find chatter zones (unstable regions) by creating an SLD and adjusting the spindle speed, depth of cut, and process settings [48].

Chatter phenomenon is part of the machine tool dynamics elements and plays a role in metal cutting since it acts as a limiting factor to productivity. Two primary techniques are commonly employed to reduce chatter [49]. The chatter can be mitigated by using the auxiliary passive or active device in the tool holder [50] or applying piezoelectric devices [51]. The second method used for chatter suppression is based on the predicted stability lobe diagram (SLD) [52] Figure 13.

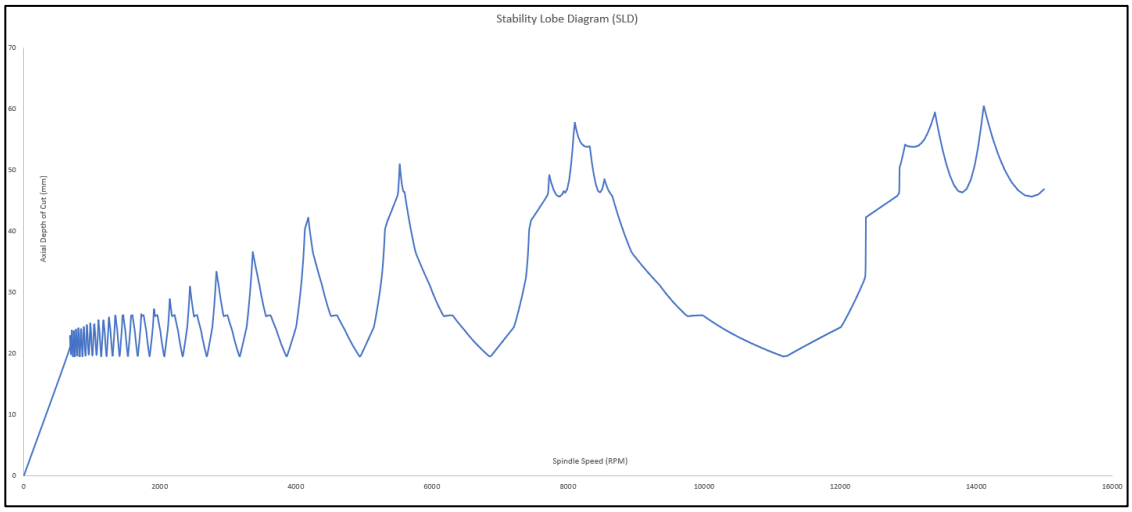

Figure 13: Stability Lobe Diagram (SLD)

The machining milling system consists of multiple components. The cutting tool, tool holder, machine spindle, part fixture and its' geometry. To obtain SLD, FRF of the tool-holder-spindle is needed, and dynamical parameters of the machining are determined by hammer impact tests - tap test equipment [53] is done to select stable machining parameters for increased productivity without expensive trial and error. In order to measure the tool tip FRF during the tap testing method, an instrumented hammer is used to excite the tool with a specified force,

and a low-mass piezoelectric accelerometer is used to measure the accompanying vibration response. The Fourier transform is used to transfer these time responses to the frequency domain, and the response to force ratio is computed. Both the x and y directions were used to perform the measurement Figure 14.

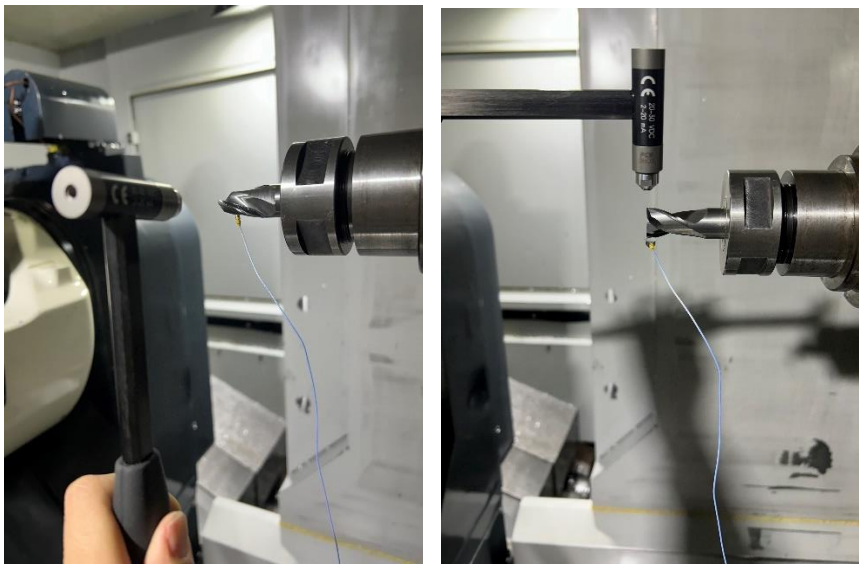

Figure 14: Tap Test instrumented hammer excites the tool tip.

Once it has identified the tool tip dynamics, it is possible to obtain a stability map, and based on the stability map, optimized machining conditions can be selected.

2.7 CUTTING PARAMETERS OPTIMIZATION

It is important to observe that the vibration directly affects the roughness of the workpiece, therefore its analysis is fundamental for this work. In cases where surface precision is required, it is important to operate in stable conditions and with adequate tool overhang [54][55].

Research has been done to compare different methods to increase the stable zone of the SLD, and/or to use optimized parameters to operate only in stable zones of the diagram. When operating in unstable zones the roughness is severely compromised. However, there is a lack of studies focussed on analyzing the impact of operating under different speeds well below the stability limit in the region of b_{lim}. The purpose of this study is to assess if there are opportunities to tune the spindle speed to realize low levels of vibration which improve surface finish and tool / machine life.

CHAPTER 3 – METHODOLOGY

In this chapter, the test procedure combined with cutting parameter selection methodology and experimental works are presented.

Firstly, the tap test was performed on the tool in order to obtain the FRF of the system. With the dynamic and geometrical properties of the tool and the definition of the workpiece material, it is possible to generate the Stability Lobes Diagram using the CutPro software. The software uses the theory already described in section 2.6, that uses the FRF of the tool and estimation of cutting force coefficients to identify the depths of cut and spindle speeds which generates a stable cut. Forces are measured using a dynamometer, and the accelerations are measured with accelerometers positioned on the workpiece and on the spindle housing. The surface roughness of the machined surface was obtained using the Alicona microscope. A schematic model including the steps of the experimental procedure is shown in Figure 15.

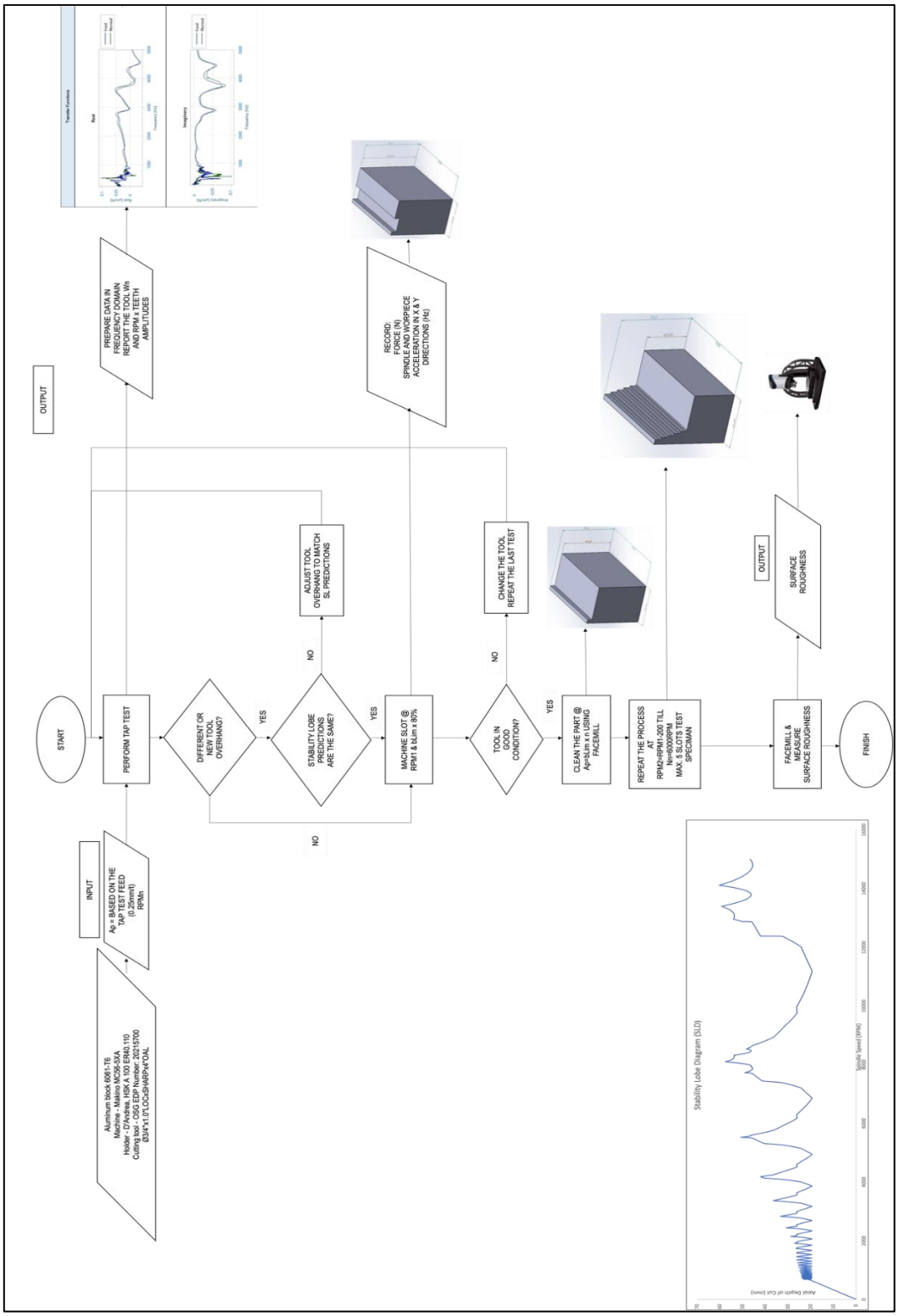

Figure 15: Experimental Procedure.

This study employs a systematic approach to machining, which includes the following steps:

Tool and Holder Selection: The first step involves selecting the appropriate cutting tool and holder. This selection is guided by the cutting parameters recommended by the Original Equipment Manufacturer (OEM).

Endmill Adjustment: Once the tool and holder are selected, the endmill is adjusted to the desired extension from the holder.

Machine Warm-Up: Prior to any machining process, the machine is warmed up to ensure optimal performance.

Tap Test and Stability Lobe Diagram (SLD) Generation: A tap test is conducted to obtain the Frequency Response Function (FRF). The FRF, defined as the ratio of response to excitation as a function of the excitation frequency, is used to generate the predicted SLD.

Depth of Cut and RPM Selection: Using the SLD, a stable axial depth of cut and Revolutions Per Minute (RPM) are selected. This includes considerations for SLDP, SLDV, and SVDR RPMs.

Slot Machining: Finally, a slot is machined at the selected RPM and axial depth of cut (b_{lim}).

This methodology ensures a systematic and efficient approach to machining, leading to optimal results. It is important to note that each step is crucial and skipping any step can lead to suboptimal outcomes.

The workpiece and accelerometers to measure acceleration in x, y, z direction experimental set-up shown in Figure 16.

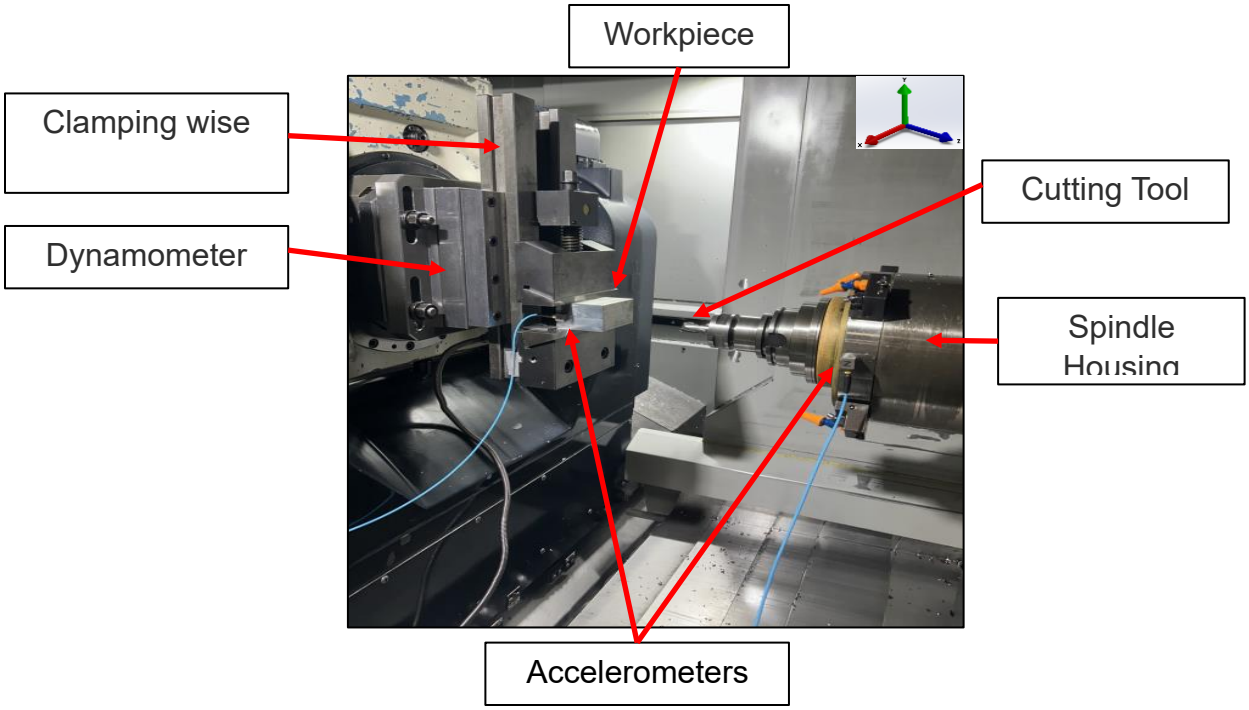

Figure 16: Workpiece and accelerometers to measure acceleration in x, y, z direction experimental set-up.

The selected workpiece material is a rectangular block of 6061 – T6 aluminum with dimensions of 31.75mm x 50.8mm x 101.6mm. The workpiece was securely clamped, with 16mm of it inserted into the vise, as illustrated in Figure 16. The cutting tests were conducted in the machine direction along the “x” axis.

3.1 CUTTING TOOL CHARACTERIZATION

The cutting tool chosen for this experiment is an OSG EXOCARB® AERO BLIZZARD® solid carbide endmill. This tool is sharp and square, with a diameter of Ø19.05mm. It features 2 effective teeth and a 30° helix angle. The length of the cut is 25.4mm, and the tool extends 38mm from the holder. The EDP Number for this tool is 20215700 as per Figure 17.

In addition to the cutting process, an optical analysis has been conducted using a microscope. This will allow for a detailed examination of the tool and workpiece, providing valuable insights into the machining process. This combination of practical application and detailed analysis ensures a comprehensive understanding of the tool's performance and its effects on the workpiece. The tool condition was studied after every cut to ensure its' integrity.

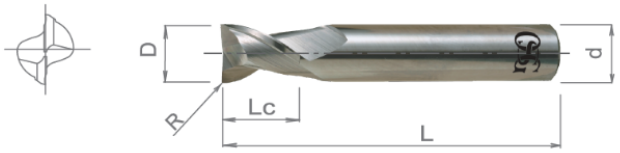

EDP Number		20215700
Mill Diameter	D	3/4
Corner Radius	R	-
Overall Length	L	4
Length of Cut	Lc	1
Shank Diameter	d	3/4
Number of Flutes		2
Milling Diameter Tolerance		+0 / -0.002"
Radius Tolerance		-

Figure 17: Cutting tool configuration.

3.2 TAP TEST

The tool frequency response function - FRF of the tool–holder–spindle system as a fixed structure and geometry shape, is essential to predict chatter vibration in milling, therefore, it was measured by the tap test [56][57][58][59][60][61][62][63][64].

The equipment for the tap test used is shown in Table 3.

ITEM DESCRIPTION	ITEM SPECIFICATION
PCB Piezotronics hammer	PCB 086C01-SN 47227- sensitivity 10.55 mV/N.
Accelerometer	PCB 352A21-SN LW268931 - sensitivity 10.55mV/g
Tap Test Software	CutPro Version AF60
DAQ card	DAQ card- NI 9234
Data acquisition software	Data acquisition software- LabVIEW 2014

Table 3: Tap test equipment.

Experimental apparatus for detecting FRFs of the tool-holder-spindle system in a machining operation is shown in Figure 18.

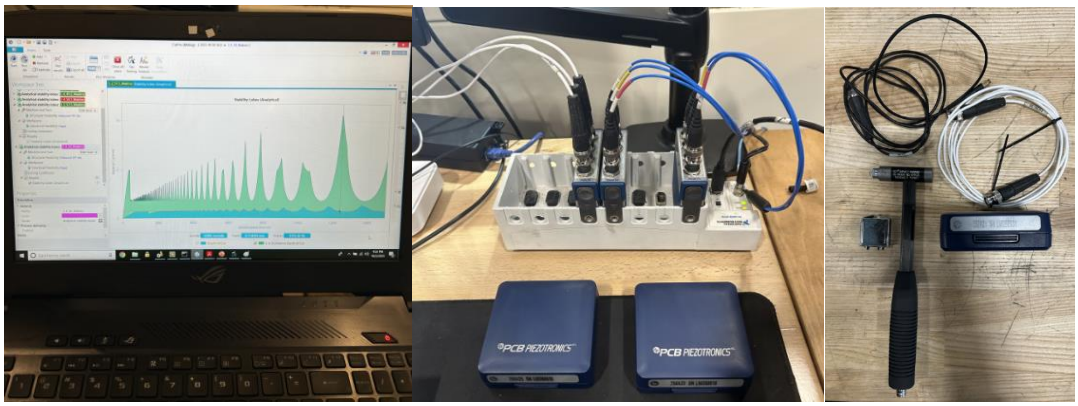

(a) (b) (c)

Figure 18:Experimental equipment for hammer impact test, (a) desktop,(b) hardware and accelerometers, (c) hammer.

The tool tip FRF was determined by tap testing, in which the tooltip was excited with a known force using an instrumented hammer (Figure 18(c)), and the resulting vibration response was recorded using a low-mass accelerometer (Figure 18(b)). The Fourier transform is used to translate these time responses to the frequency domain, and the resulting ratio of the force response is computed, as seen in Figure 18(a). As shown in Figure 19, the measurement was carried out in both the x and y directions.

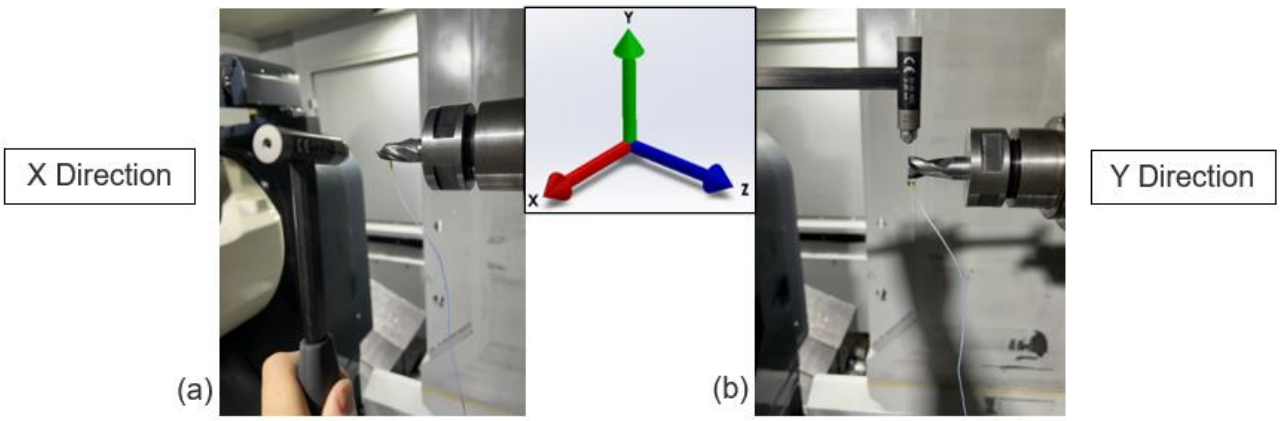

Figure 19: Tap test measurement in x (a) and y (b) directions.

The piezotronics accelerometer was installed at the tool's tip. Prior to conducting the tap testing, the machine underwent a warm-up period of one hour to ensure the bearings were warmed up.

3.3 CUTTING TESTS

The cutting conditions were established as follows:

1. Workpiece Material: The material selected was aluminum alloy 6061-T6, which is extensively used in aerospace, automotive, maritime, and structural industries due to its versatility in heat treatment. It boasts a high degree of hardness, an excellent weight-to-strength ratio, corrosion resistance, and superior forming properties. The hardness of 58±1 HRB was verified using a Hardness Tester.

2. Cutting Approach: Full slot cuts were performed to ensure a stable cut. A constant axial depth of cut (ap = b) of 8mm was maintained.

3. RPM Selection: RPMs were chosen based on the Stability Lobe Diagram (SLD), with picks, valleys, and random RPMs selected.

4. Feed per Tooth: A feed per tooth of 0.25mm was selected, following the recommendation of the tool supplier.

5. Surface Roughness Measurements: Both up-milling and down-milling surface roughness measurements were conducted.

6. Machining Operation: The cutting tests were performed on a Makino MC56-5XA CNC horizontal machining center, with all cuts performed with motion in the "x" direction.

7. Accelerometer Installation: A tri-axial accelerometer was installed directly on the part at the same location to capture the force, workpiece, and spindle housing acceleration.

The equipment used for these processes is detailed in Table 4 and Figure 20.

ITEM DESCRIPTION	ITEM SPECIFICATION
Dynamometer	Kistler dynamometer 9255B
PCB Piezotronics Accelerometer housing	PCB, ICP®, TRIAXIAL-356A25-sensitivity(mV/g): 24.57mV/g (X), sensitivity 24.58mV/g (Y), sensitivity 24.42mV/g (Z)
PCB Piezotronics Accelerometer workpiece	PCB Piezotronics 356A25, Sensitivity(mV/g): X = 24.62; Y = 24.88; Z = 24.69
Amplifier	Kistler type 5010 Dual Mode amplifier (Figure 20 (a)) (Transducer sensitivity 7.86 mV/MU and scale 500 MU/Volt)
DAQ card	NI 9234 (Figure 20 (b))
Data acquisition software	LabVIEW 2014 (Figure 20 (c))

Table 4: Force, workpiece, and spindle housing acceleration equipment.

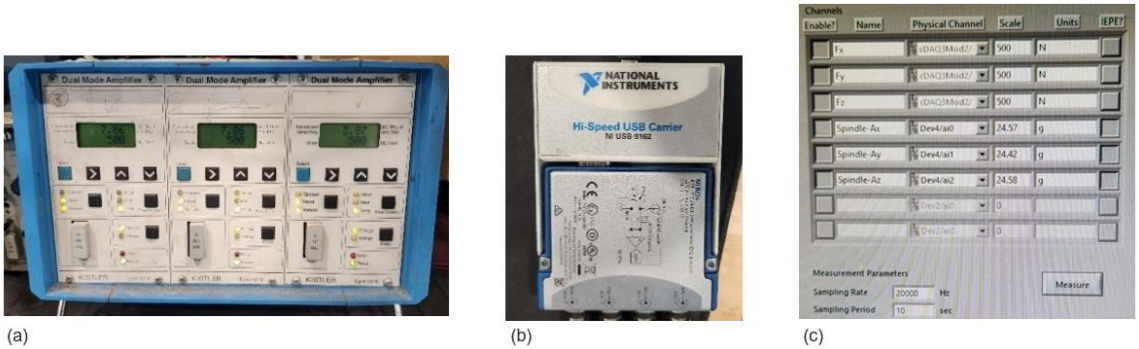

Figure 20: (a) Dynamometer Amplifier. (b) DAQ card. (c) Test Setup-Labview accelerometers data.

3.3.1 SURFACE ROUGHNESS

The measurement of surface roughness was conducted using a Mitutoyo surface roughness instrument (Mitutoyo SJ-201) and an Alicona Infinite Focus confocal microscope (Model G5Vc3). A visual representation of the two surface testers used can be found in Figure 21. The roughness parameters were computed in accordance with the standards set forth in DIN EN ISO 4287:1998 and DIN EN ISO 4288:1998 [40].

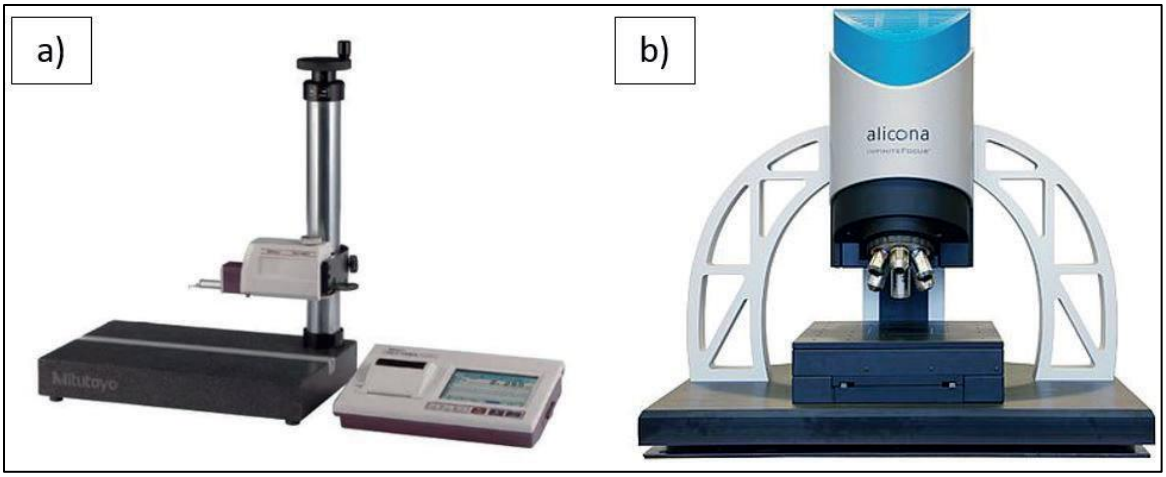

Figure 21 - (a) Mitutoyo SJ-201 contact profilometer, (b) Alicona Infinite Focus confocal microscope.

CHAPTER 4 – RESULTS AND DISCUSSION

4.1 TAP TEST MODAL DATA ANALYSIS

As mentioned in literature review section 2.6, to investigate cutting chatter problems, a milling Stability Lobe Diagram is typically constructed. Finding the ideal cutting parameters in a stable area is the goal [65].

The thesis hypothesis was that at the depth of cut that is well under b_{lim} of SLD, the surface finish will vary depending on the cutting speed aligning with the valleys and peaks of the SLD. Tap tests were performed in the same tool with 3 different overhangs. The tool with the shortest overhang (Figure 22) was selected as it has the highest rigidity which ensure the most stable cut.

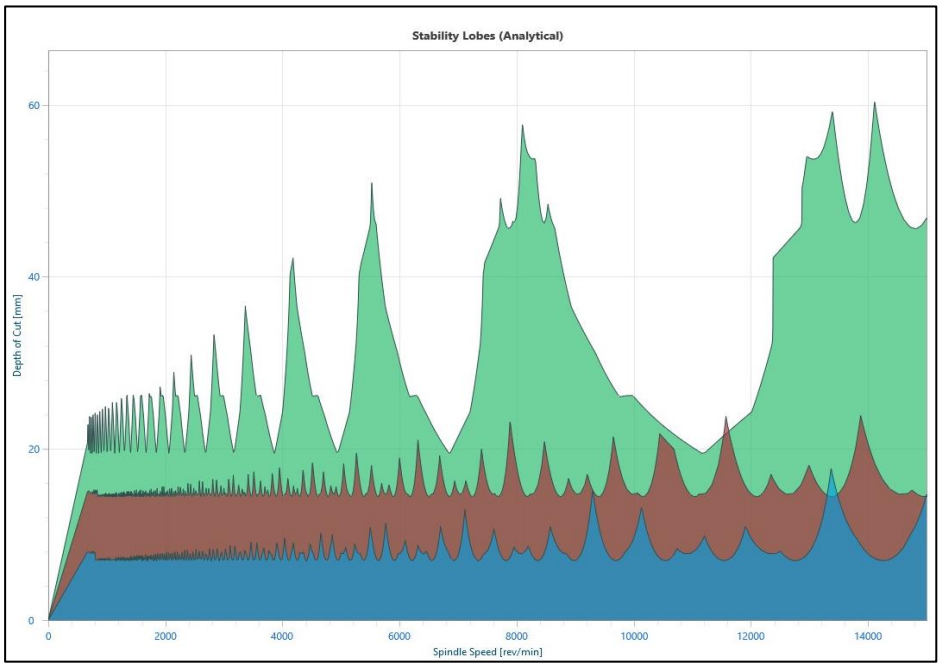

Figure 22: SLD of 3 tools. Blue 55mm extension, Brown 47mm extension, Green 38mm extension.

The modal analysis and natural frequency identification from the tap-test was performed based on the Cutpro guide [66]. The dominant tool natural frequency was identified around 550Hz.

The FRFs measured at the tip of the tool are measured in X and Y directions as described in section 3.2, and are shown in Figures 23 and 24 with fitted curves.

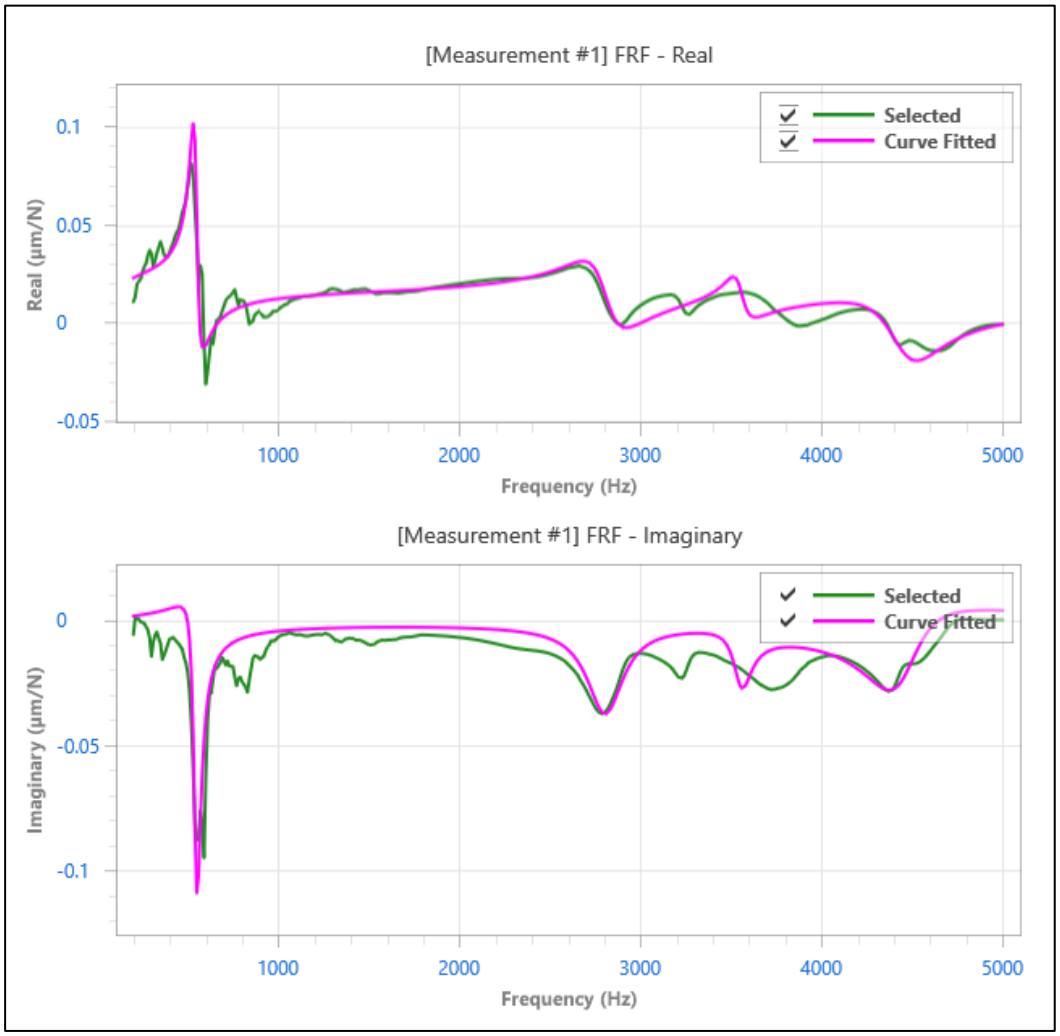

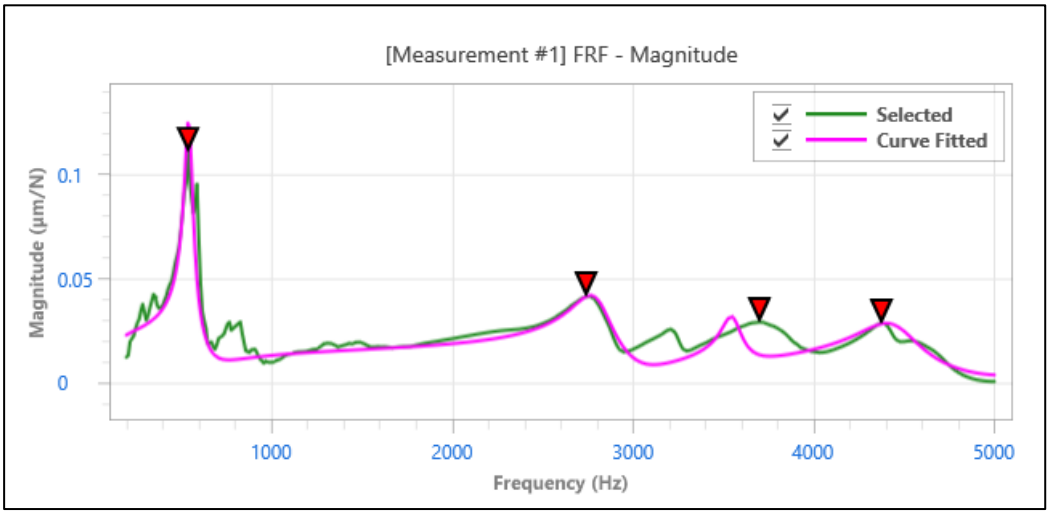

Figure 23: Frequency Response Function in X direction.

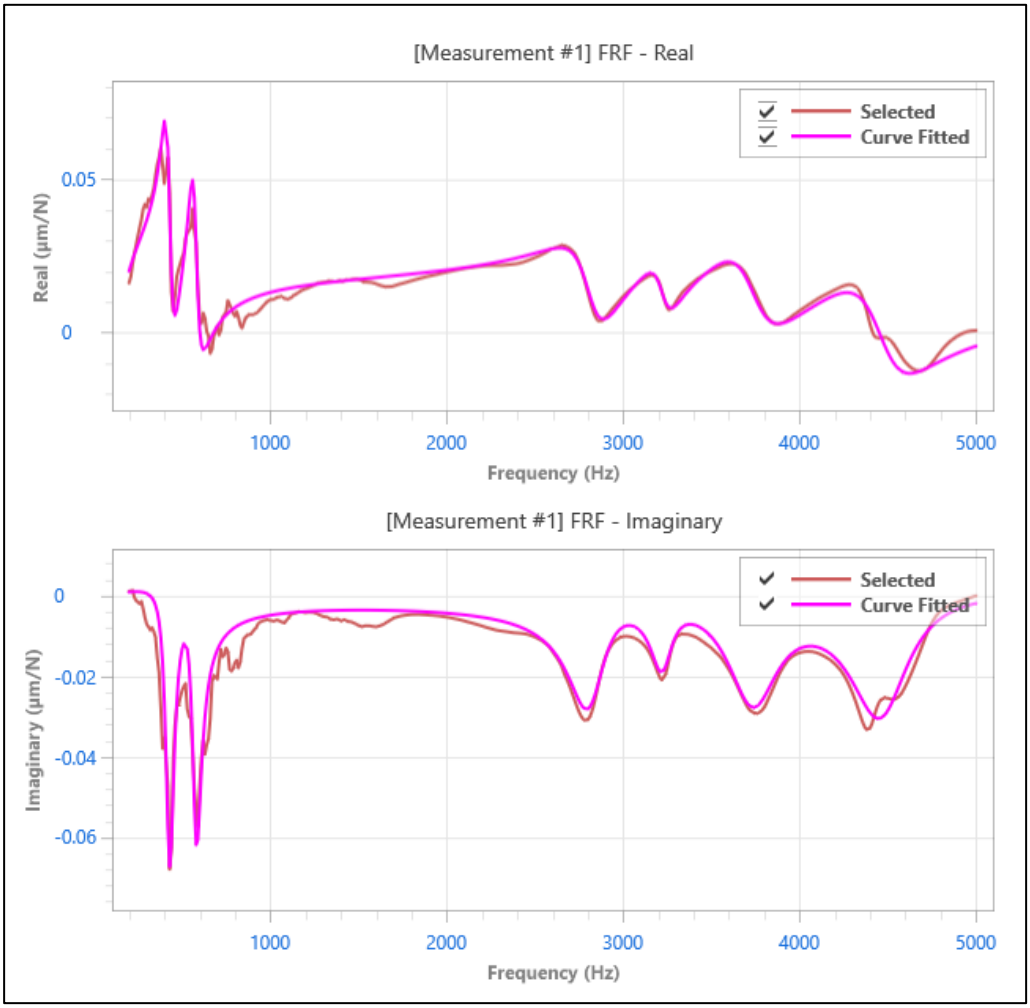

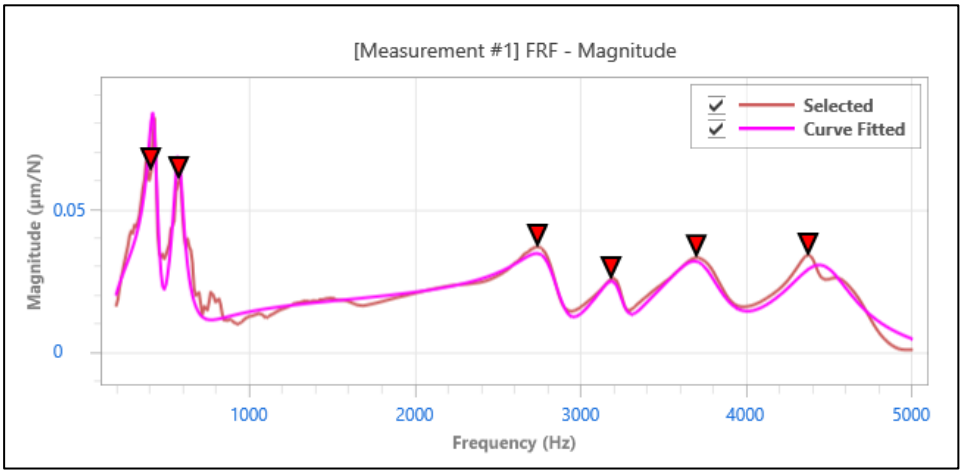

Figure 24: Frequency Response Function in Y direction.

The modal parameters are shown in tables 5 and 6.

X-direction

Mode No	Frequency [Hz]	Damping Ratio [%]	Modal Stiffness [N/m]	Modal Mass [kg]
1	547.0969	4.4206	1.11E+08	9.3979E+00
2	2810.0155	4.363	3.29E+08	1.0564E+00
3	3553.5107	1.7088	1.43E+09	2.8739E+00
4	4452.8609	4.1197	5.34E+08	6.8219E-01

Table 5: Generated curve-fit modal parameters for the X-direction.

Y-direction

Mode No:	Frequency[Hz]	Damping Ratio [%]	Modal Stiffness [N/m]	Modal Mass [kg]
1	429.3175	6.719	1.09E+08	1.4919E+01
2	577.0424	5.3202	1.79E+08	1.3580E+01
3	2823.5778	4.4283	4.86E+08	1.5452E+00
4	3226.7949	2.346	1.37E+09	3.3337E+00
5	3739.6885	4.6452	4.22E+08	7.6442E-01
6	4471.2261	4.4998	3.75E+08	4.7484E-01

Table 6: Generated curve-fit modal parameters for the Y-direction.

The difference between X and Y directions is noticeable, showing that dynamics of the system are not symmetrical due to the presence of the gullets within the flutes of the tool.

The resulting stability lobe are shown in Figure 25.

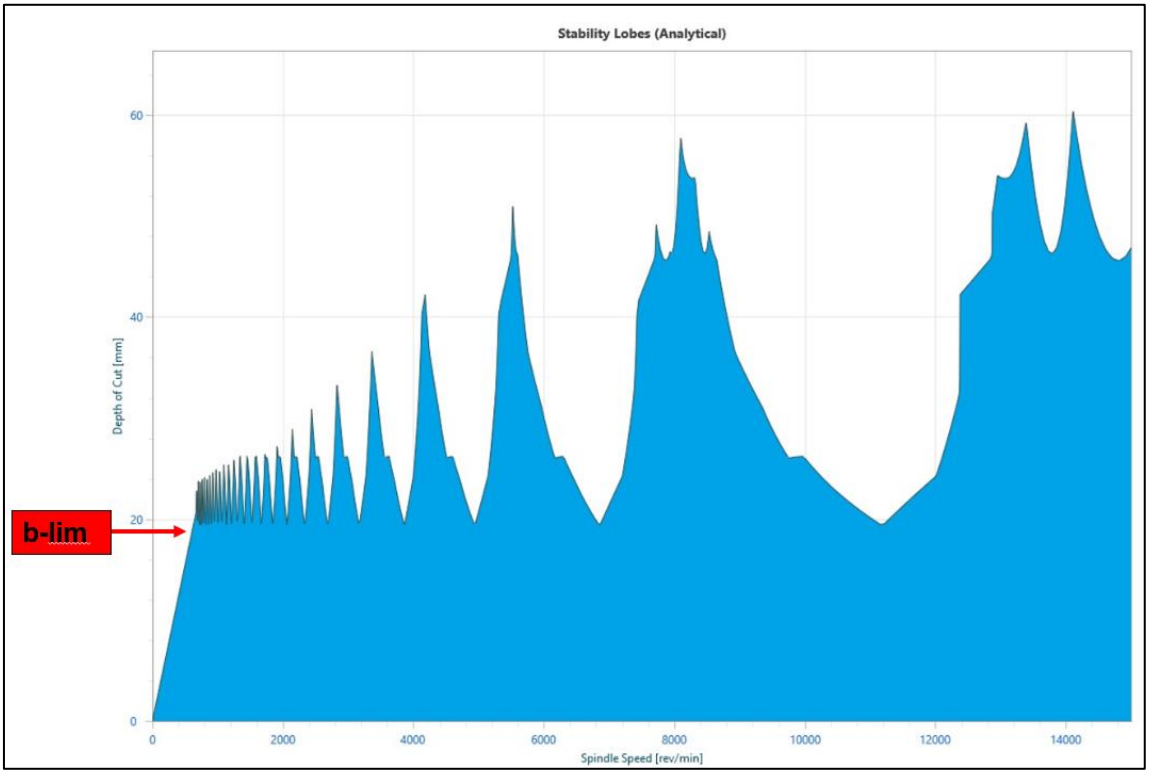

Figure 25: Stability lobes diagram for Ø19.05mm endmill, 38mm overhang, Al6066-T6.

4.2 SLD vs SURFACE ROUGHNESS (Ra) DATA ANALYSIS

There was a total of 40 cuts performed according to section 3.3. With 20 cuts performed as up-milling and 20 cuts as down-milling. Acceleration result measurements at frequency domain @ 5535RPM are shown in Figure 26 to validate the results.

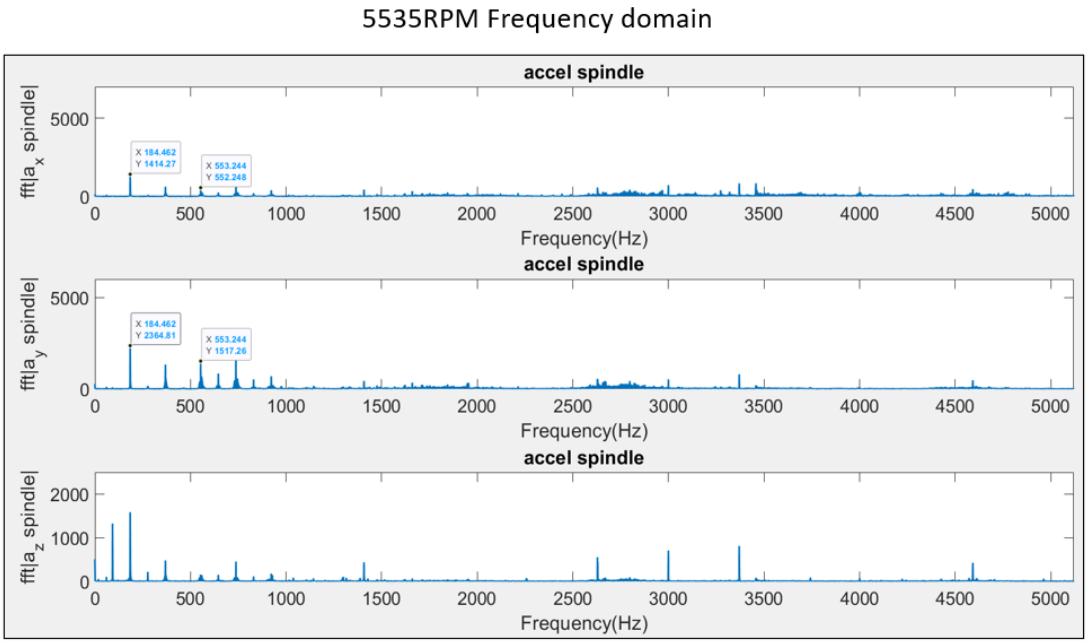

Figure 26: Acceleration result measurements in the frequency domain for a spindle speed of 5535 RPM.

Equation (5) was used to validate the data collected.

Spindle Frequency excitement = 5535 / 60 x 2 = 184.5Hz

Natural Frequency excitement = 550Hz

For the experiment, 10 blocks of aluminum were used. Every piece had 4 cuts. After the blocks were machined, they were cut in half on a bandsaw to have access to the machined surface for the Alicona measurements. Every block was scribed with identifying marks and every slot was properly identified. In addition, cutting forces, spindle and workpiece accelerations have been captured and recorded to match the part identifiers.

Surface roughness measurements were taken using the Alicona as per Figure 27.

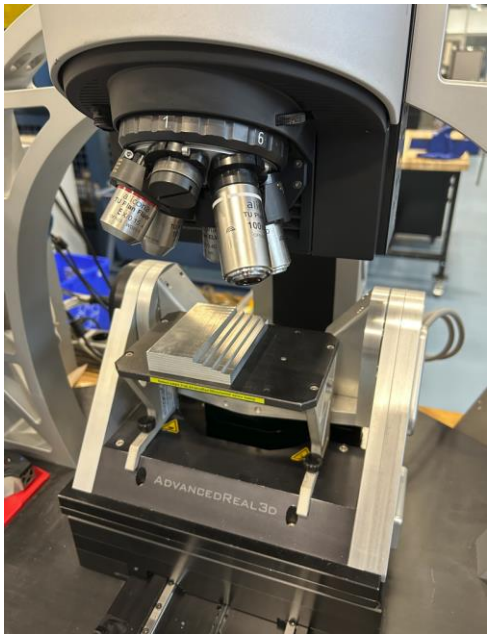

Figure 27: Figure Workpiece set-up in Alicona.

Every slot was measured in 3 locations as per Figure 28.

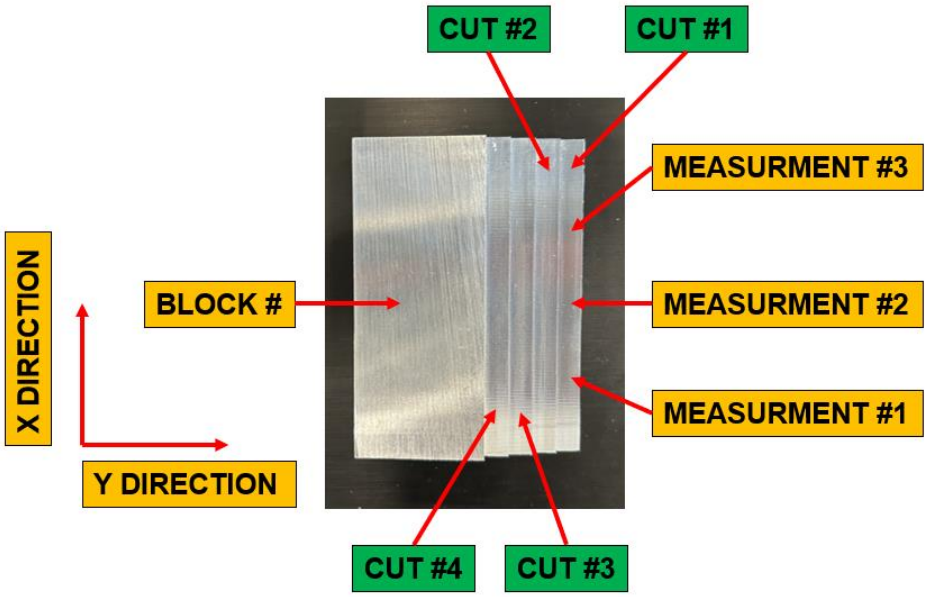

Figure 28: Measurements location.

Every roughness measurement was performed three times for X and Y directions as shown in Figure 29.

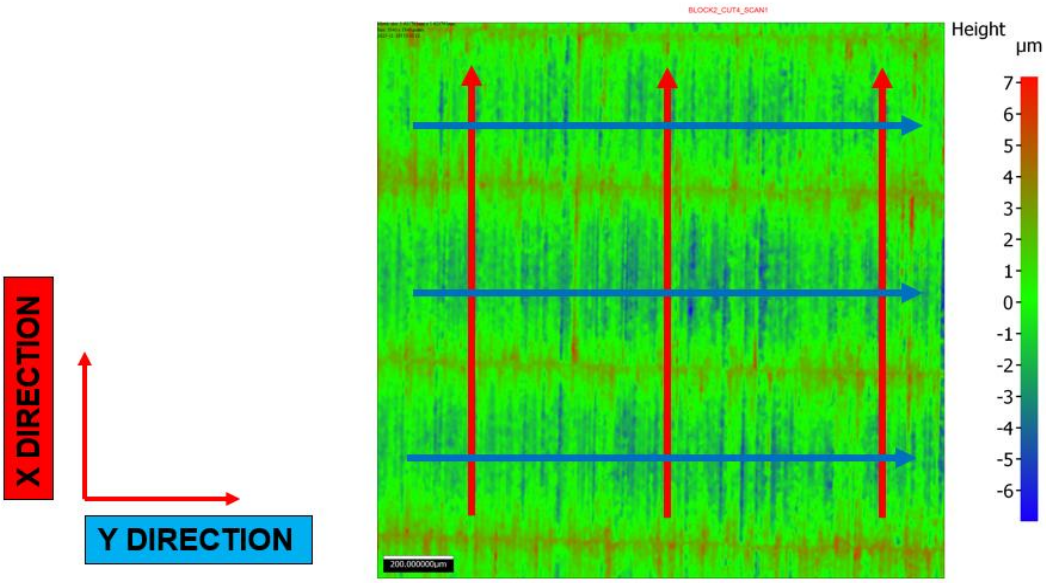

Figure 29: Alicona measurements pattern.

Every slot had in total of 9 scans in X and Y directions. The average number of the surface roughness measurements is shown in Table 7.

BLOCK #	CUT #	SCAN #	DIRECTION	MEASURMENT #	SURFACE ROUGHNESS	
1	1	1	X	1	0.73384	
				2	0.681558	
				3	0.801856	
		2		1	0.54581	
				2	0.665167	
				3	0.71662	
		3		1	0.847601	
				2	0.859711	
				3	0.728554	0.731191
		1	Y	1	0.614238	
				2	0.618753	
				3	0.692088	
		2		1	0.67289	
				2	0.664594	
				3	0.627859	
		3		1	0.632496	
				2	0.602076	
				3	0.606605	0.636844

AVERAGE IN X DIRECTION

AVERAGE IN Y DIRECTION

Table 7: Surface roughness measurement table matrix.

In total, there were 10 (blocks) x 4 (slots) x 2 (X & Y directions) x 9 (scans) = 720 scans performed to collect the surface roughness from 40 machined surfaces. The roughness data comparing the results on Peaks and Valleys is presented. Surface roughness for each RPM used for down-milling cuts are shown in Table 8.

Block #	Cut #	Material	Al 6061-T6			Surface Roughness	
		Hardness	58±1HRB			3D Alicona	
		Cut type	Stability Type	RPM	Feed	X direction	Y direction
6	1	Down-Milling	SLDP	4180	2090	0.766	0.577
6	2	Down-Milling	SVDV	4950	2475	0.725	0.443
6	3	Down-Milling	SLDP	5535	2768	0.678	0.399
6	4	Down-Milling	SLDR	6000	3000	0.751	0.413
7	1	Down-Milling	SVDV	6860	3430	0.806	0.537
7	2	Down-Milling	SLDR	7500	3750	0.790	0.444
7	3	Down-Milling	SLDP	8115	4058	0.759	0.463
7	4	Down-Milling	SLDR	8885	4443	0.717	0.428
8	1	Down-Milling	SLDR	9655	4828	0.736	0.470
8	2	Down-Milling	SLDR	10425	5213	0.737	0.385
8	3	Down-Milling	SVDV	11195	5598	0.707	0.446
8	4	Down-Milling	SLDR	12200	6100	0.696	0.461
9	1	Down-Milling	SLDR	12500	6250	0.720	0.428
9	2	Down-Milling	SLDR	12750	6375	0.755	0.376
9	3	Down-Milling	SLDR	13000	6500	0.729	0.367
9	4	Down-Milling	SLDP	13400	6700	0.759	0.426
10	1	Down-Milling	SVDV	13800	6900	0.774	0.454
10	2	Down-Milling	SLDP	14115	7058	0.704	0.361
10	3	Down-Milling	SVDV	14800	7400	0.741	0.390
10	4	Down-Milling	SVDV	15000	7500	0.746	0.398
SLDR - Stability Lobe Diagram Random							
SLDP - Stability Lobe Diagram Peak							
SLPV - Stability Lobe Diagram Valley							

Table 8: Down Milling Surface Roughness.

The effect of surface roughness in different regions of the SLD can be observed in Figure 30. There is a trend for a higher roughness on valleys and lower roughness on peaks, as observed in most of the points identified with the green dashed line. The error bars identified with the light grey solid line.

- Down milling

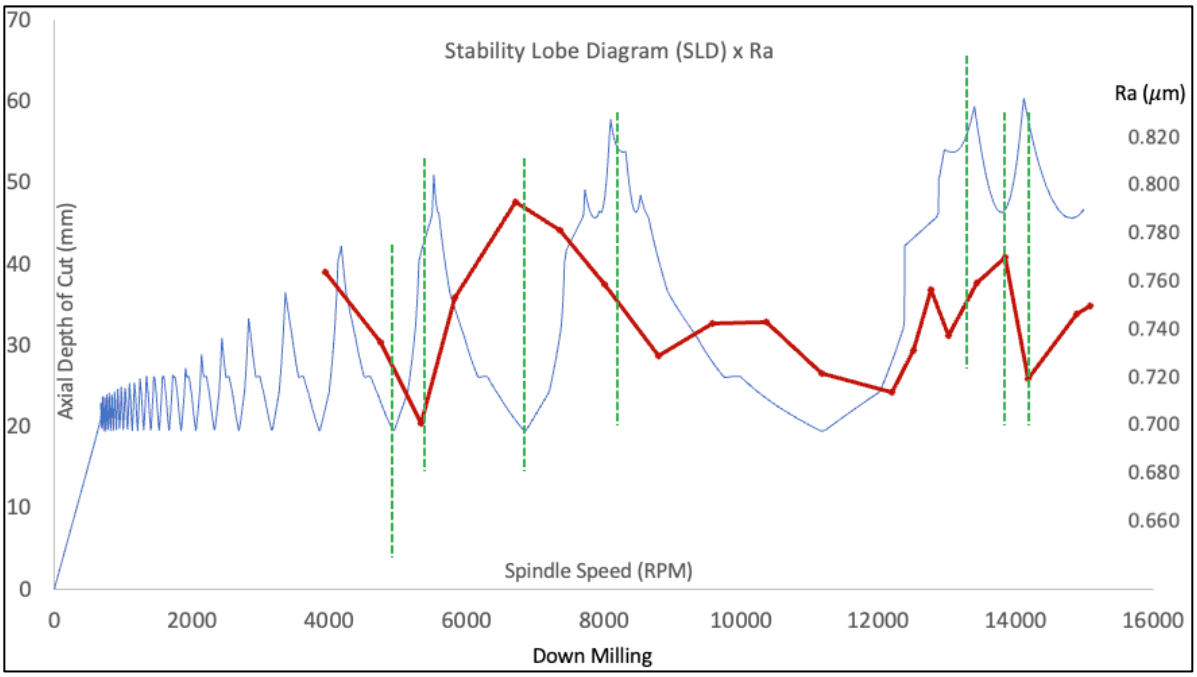

Figure 30: Stability lobe Diagram (SLD) versus Surface Roughness (Ra) Down Milling.
(The average standard deviation is 0.07)

The surface roughness for each RPM for up-milling cuts is shown in Table 9.

Block #	Cut #	Material	Al 6061-T6			Surface Roughness	
		Hardness	58±1HRB			3D Alicona	
		Cut type	Stability Type	RPM	Feed	X direction	Y direction
3	4	Up-milling	SLDP	4180	2090	0.699	0.495
3	3	Up-milling	SVDV	4950	2475	0.710	0.456
3	2	Up-milling	SLDP	5535	2768	0.709	0.502
1	1	Up-milling	SLDR	6000	3000	0.731	0.637
1	2	Up-milling	SVDV	6860	3430	0.684	0.542
5	1	Up-milling	SLDR	7500	3750	0.903	0.746
1	3	Up-milling	SLDP	8115	4058	0.711	0.537
5	3	Up-milling	SLDR	8885	4443	0.714	0.649
5	2	Up-milling	SLDR	9655	4828	0.854	0.787
5	4	Up-milling	SLDR	10425	5213	0.791	0.671
1	4	Up-milling	SVDV	11195	5598	0.740	0.689
4	1	Up-milling	SLDR	12200	6100	0.890	0.744
4	2	Up-milling	SLDR	12500	6250	0.738	0.645
4	3	Up-milling	SLDR	12750	6375	0.734	0.717
4	4	Up-milling	SLDR	13000	6500	0.731	0.571
3	1	Up-milling	SLDP	13400	6700	0.815	0.745
2	4	Up-milling	SVDV	13800	6900	0.814	0.714
2	1	Up-milling	SLDP	14115	7058	0.738	0.716
2	2	Up-milling	SVDV	14800	7400	0.824	0.781
2	3	Up-milling	SVDV	15000	7500	0.764	0.721
SLDR - Stability Lobe Diagram Random							
SLDP - Stability Lobe Diagram Peak							
SLPV - Stability Lobe Diagram Valley							

Table 9: Up-Milling Surface Roughness.

For up milling (Figure 31) the trend for a higher roughness on valleys and lower roughness on peaks is less noticeable with the data collected. Probably this is because of the friction that occurs when rubbing on the clearance face that

excites vibration in the direction of the cutting force and limits the vibration amplitude in the thrust force direction [67].

- Up milling

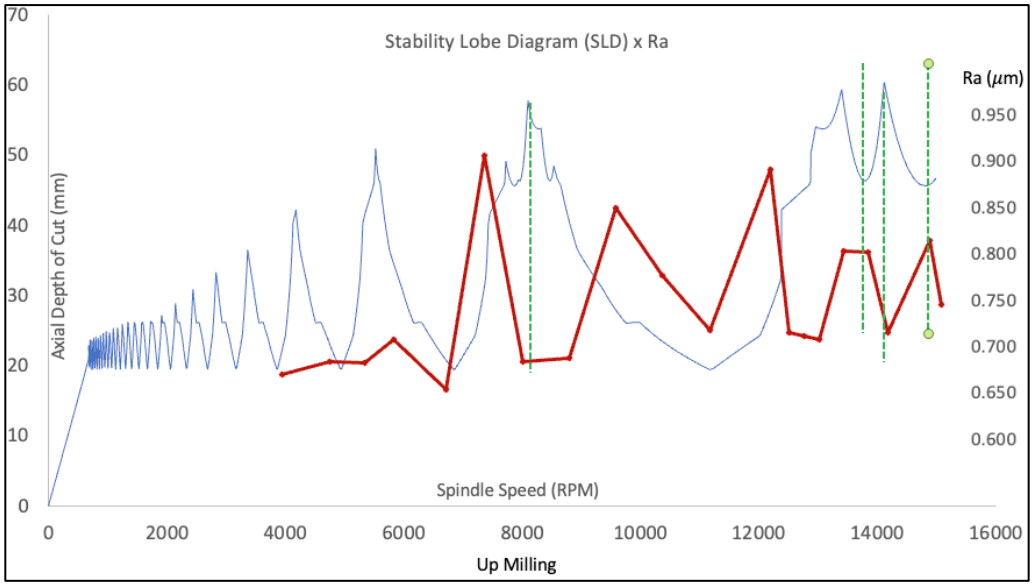

Figure 31: Stability lobe Diagram (SLD) versus Surface Roughness (Ra) Up Milling. (The average standard deviation is 0.075)

As already commented, the effects on roughness were more pronounced for down-milling operations. Therefore, from now on, the statistical analysis and after, the acceleration assessment will be conducted only for down-milling operations.

To further understand the behavior of surface roughness peaks and valleys an Analysis of Variance (ANOVA) was performed for all the data using the Minitab software. The values for mean average roughness are very close (Figure 32), but there is a trend for a higher roughness on valleys and lower roughness aligning with the peaks of SLD. This means there is an opportunity for improved surface

roughness when up milling when RPM is aligned with SLD peaks based on surface roughness Ra values taken below b_{lim}.

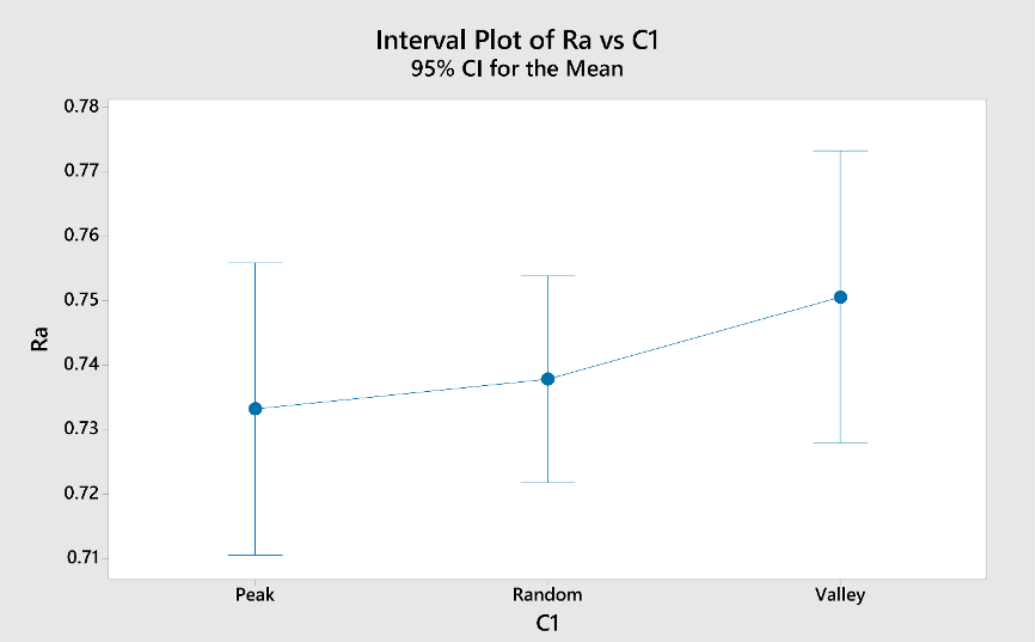

Figure 32: Anova results for significance with 95% confidence.

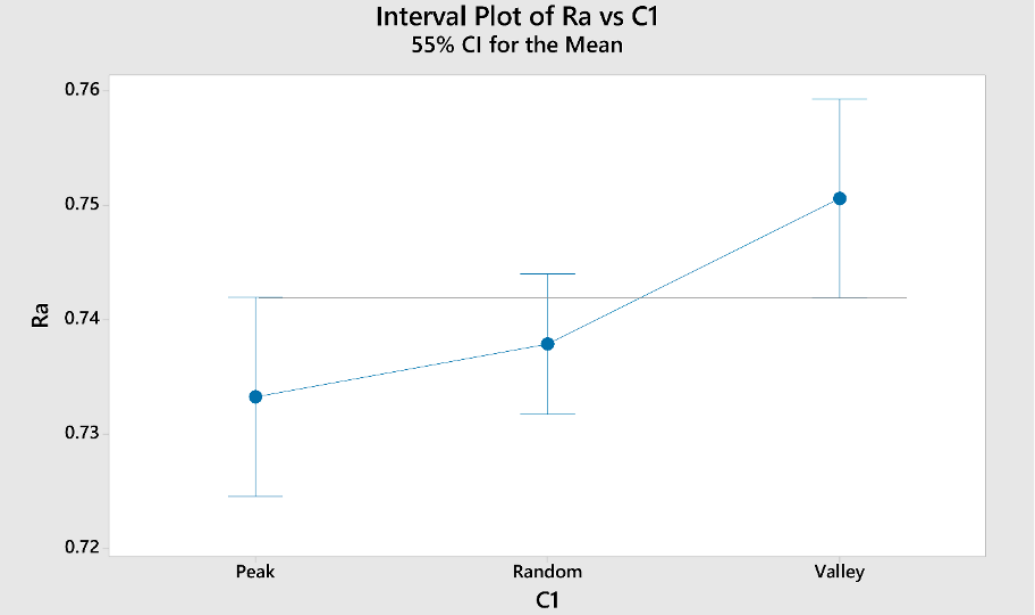

Figure 33: Anova results for significance with 55% confidence.

Analyzing the data, it is possible to observe that the values are statistically different but only at a confidence level below 55% (Figure 33). The values are close due to the stiffness of the tool since for this case the maximum depth of cut without chatter, was theoretically up to 18 mm.

In cases where the operation conditions are closer to b_{lim}, i.e., using higher depths of cut or more compliant tools, this difference should be more pronounced. However, it is important to observe that even operating under conservative conditions, with the depth of cut much lower than the limit, there is still a difference between peaks and valleys.

4.3 CUTTTING FORCE DATA ANALYSIS

The cutting force (Fy) measured for each spindle speed tested are shown in Fig 34.

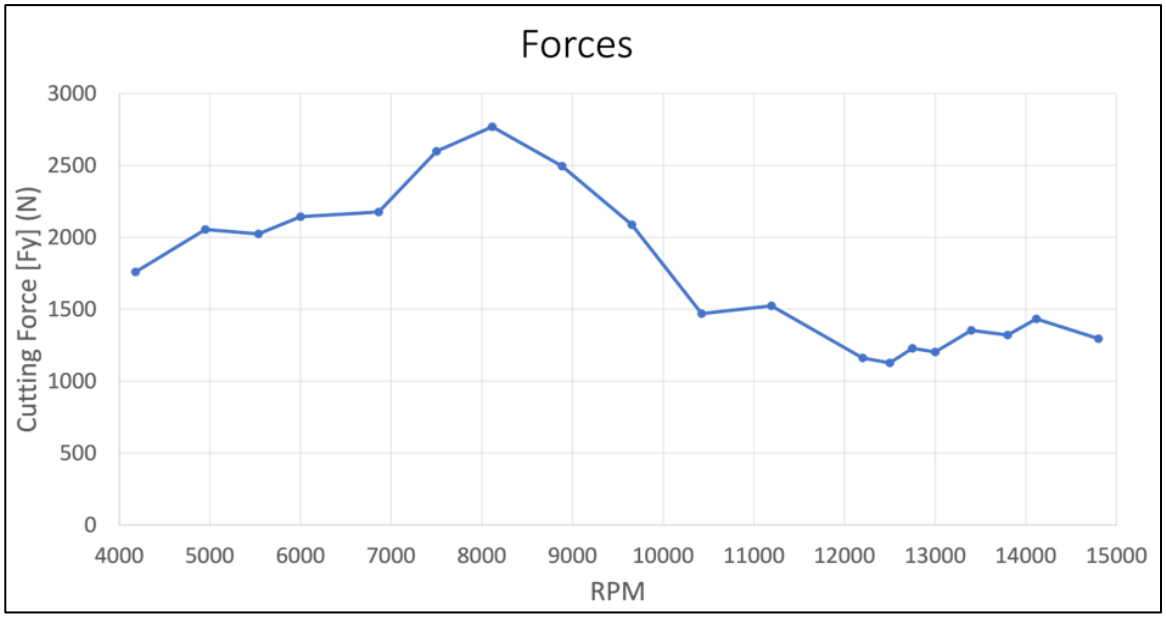

Figure 34: Cutting Forces in Y direction.

The cutting forces have a positive trend up to 8,000 RPM. After that, the forces are significantly reduced. This could have occurred due to the thermal softening of the workpiece material during cutting. With an increase in cutting speed the heat generated tends to be higher but is not dissipated through the workpiece or tool since the increase in cutting speed reduces the time available for heat dissipation. With higher heat being generated and lower dissipation, the temperature of the chip tends to increase with the heat leaving the cutting zone with the chip [68].

The increase in temperature can lead to thermal softening of the workpiece surface, this could reduce the tensile strength, yield strength, and hardness of the material. With this, the shearing force necessary to plastically deform the material is lower and, therefore, cutting forces should also be lower [68].

Thus, it is very important to keep in mind that comparing forces for significantly different RPMs in peaks and valleys could be affected by this phenomenon.

4.4 ACCELERATION ANALYSIS

The roughness difference between peaks and valleys could be explained by analyzing the acceleration of the spindle and/or workpiece. A higher variation of acceleration peaks tends to result in a higher surface roughness.

Figure 35 shows an example of one of the acquisitions using accelerometers on the workpiece and on the spindle, respectively.

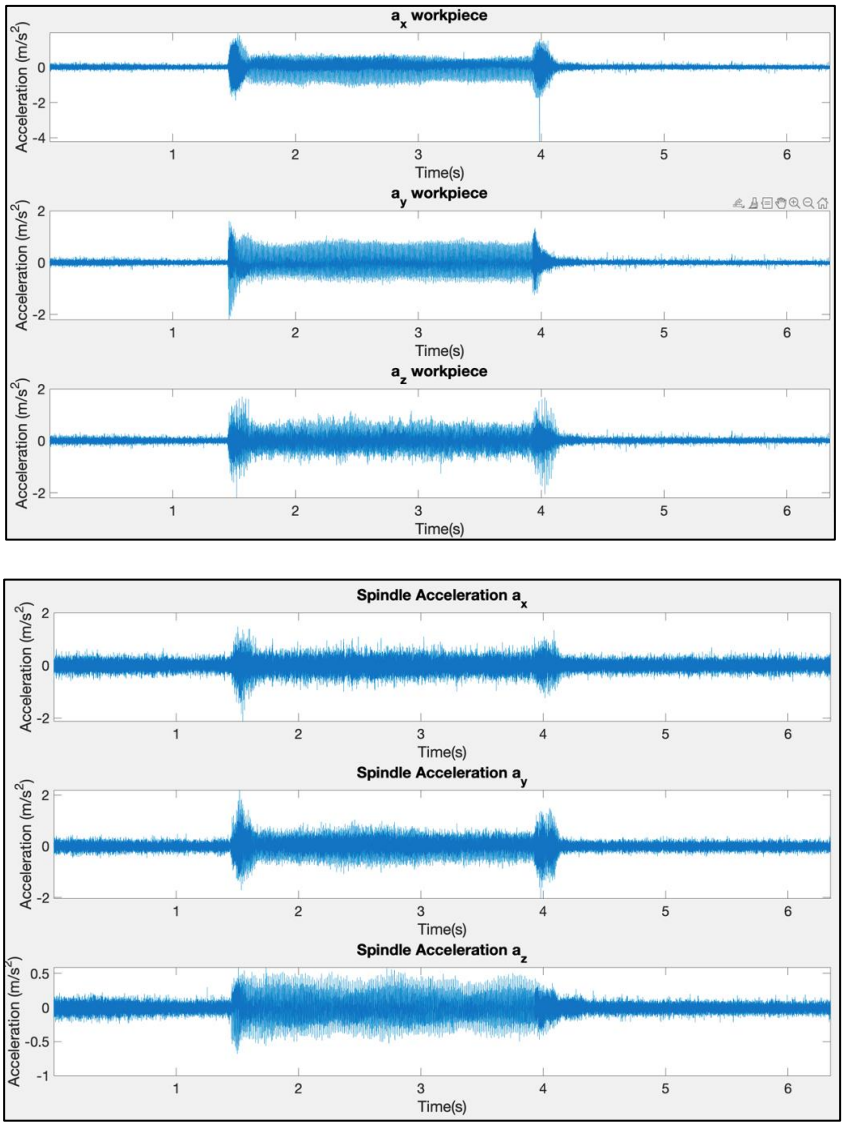

Figure 35: Vibration data from accelerometers on the workpiece and on the spindle.

As can be seen, the spindle acceleration has a significant noise level. Therefore, workpiece acceleration was used for the analysis. Only the stable regions of cut were considered during the accelerations analysis. This means that values on the entrance and the exit of the tool were not considered.

In order to understand the effect of acceleration on surface roughness, the points with the highest variation in surface roughness between peaks and valleys were chosen. Figure 36 shows the regions chosen for the analysis (black circles).

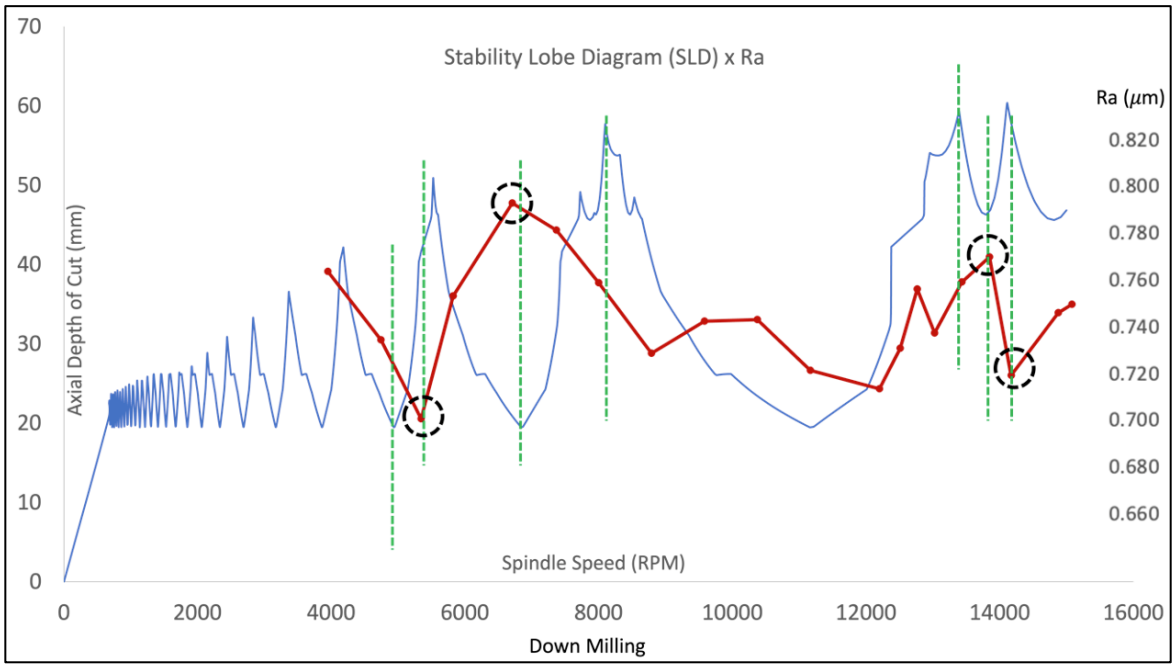

Figure 36: Down Milling Surface Roughness VS RPM.

It's important to take into account the effect of cutting speed on different mechanisms during machining, as commented in the cutting force analysis section. Therefore, comparisons were made between similar cutting speed values.

The first comparison was made between 5,535 RPM (Peak) and 6,860 RPM (Valley). As already mentioned, it is expected that the peak regions present lower roughness and lower vibration levels, since it is in a more stable zone. Figure 37 shows the accelerations in x, y and z for peak at 5,535 RPM and Figure 38 shows accelerations in x, y and z for valley at 6,860 RPM.

Peak – 5,535 RPM

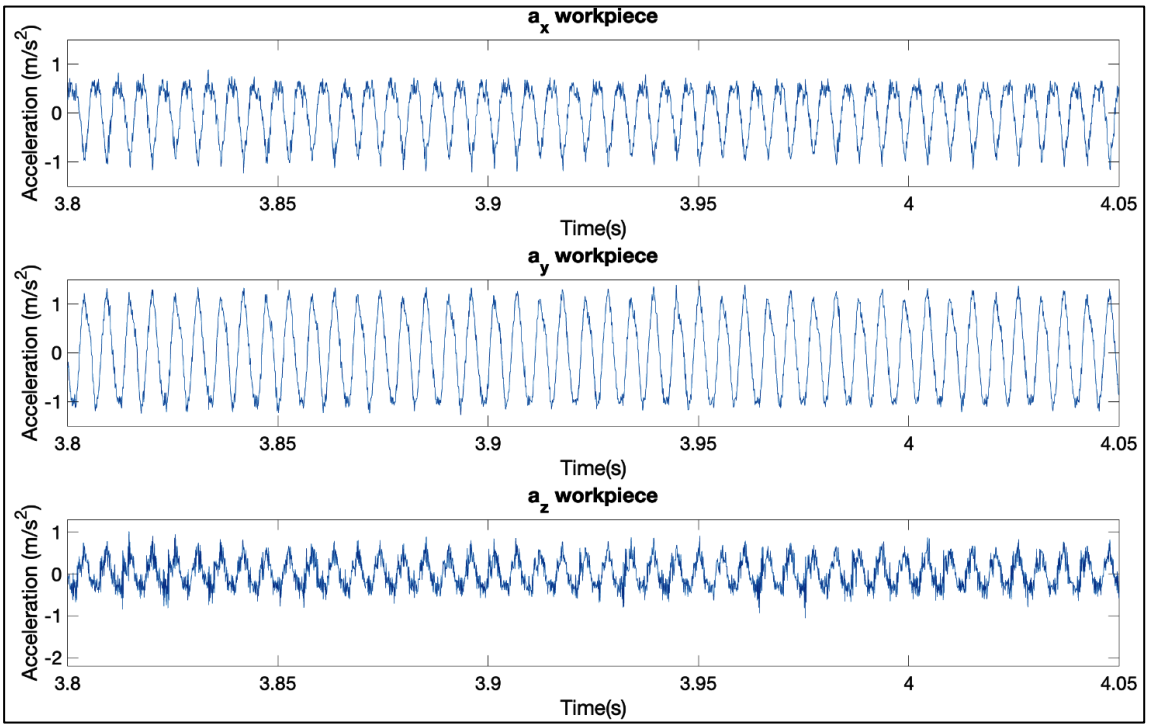

Figure 37: Accelerations in x, y and z for Peak 5,535 RPM.

Valley – 6860 RPM

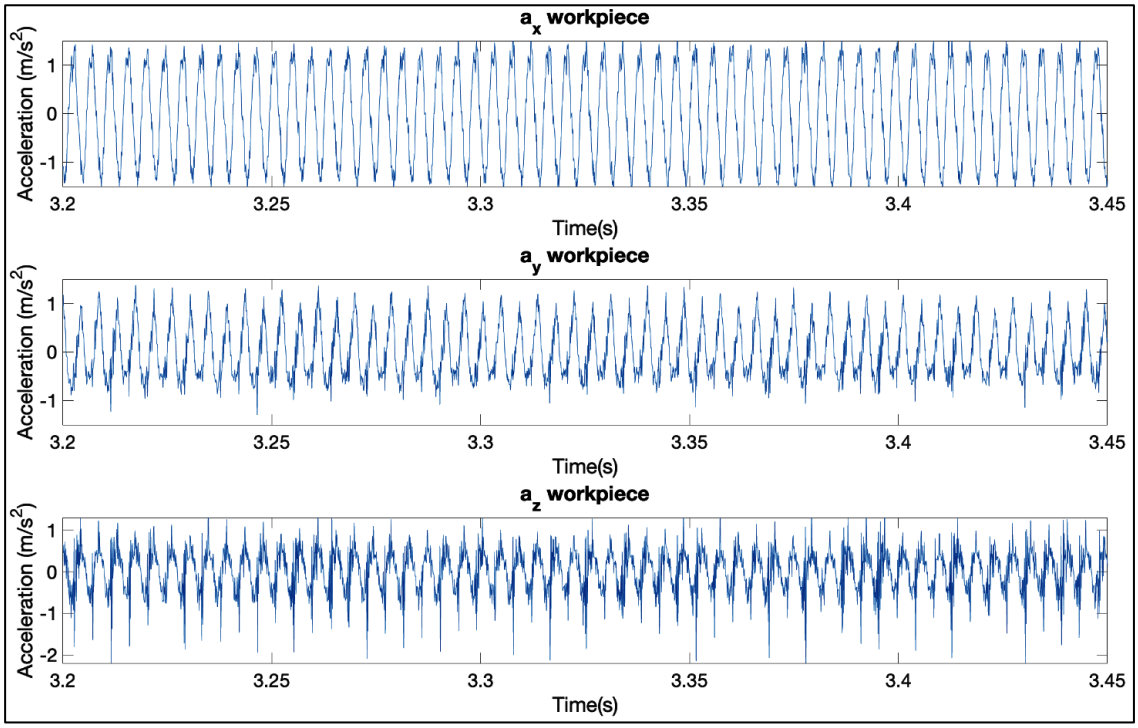

Figure 38: Accelerations in x, y and z for Valley 6,860 RPM.

To observe how the vibration is affecting the surface roughness it is necessary to analyze the difference between acceleration peaks since this is what is going to directly affect the surface. Figure 39 and Figure 40 show the same comparison but analyzing a shorter time period. With this, it is possible to observe the force variation in a more detailed way.

Peak – 5,535 RPM

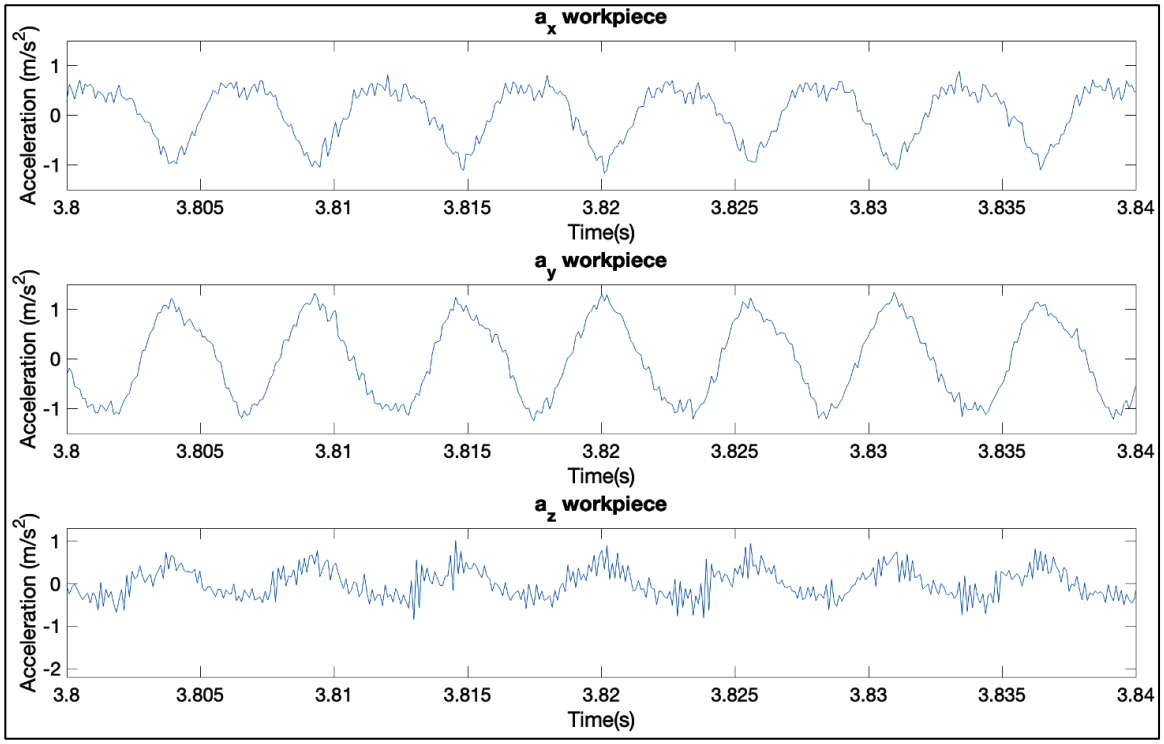

Figure 39: Zoomed accelerations in x, y and z for Peak 5,535 RPM.

Valley – 6,860 RPM

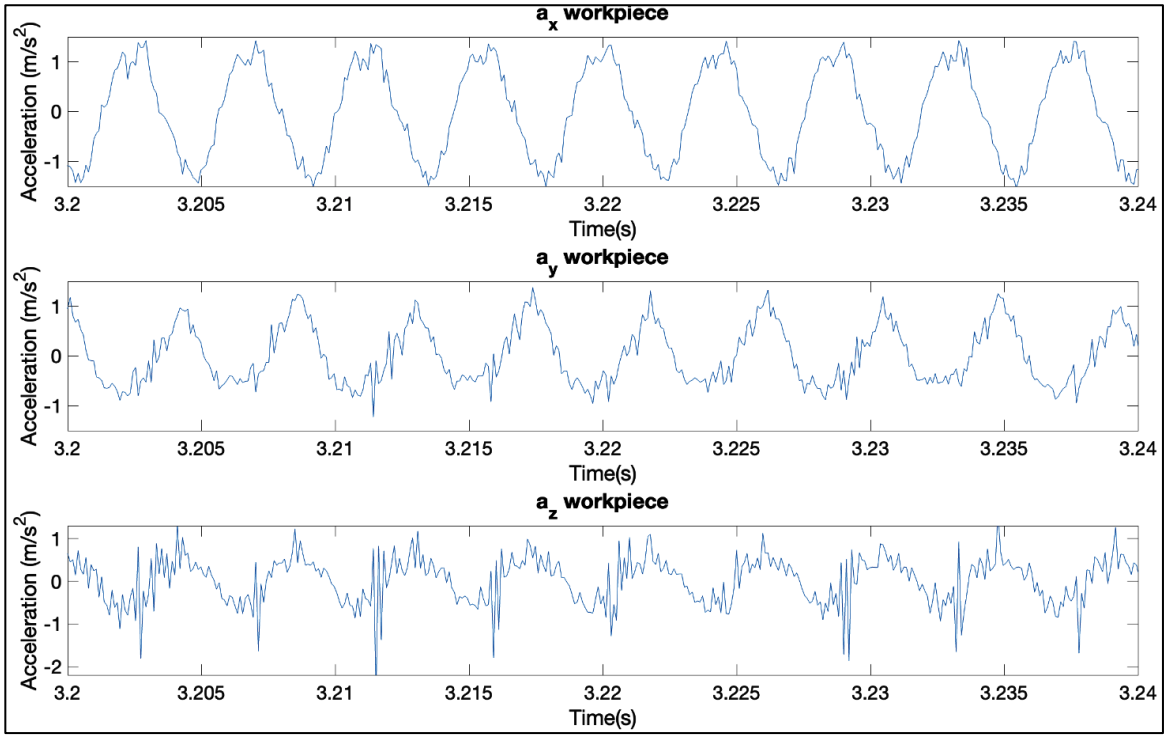

Figure 40: Zoomed accelerations in x, y and z for Valley 6,860 RPM.

It is noticeable that in the valley region, the accelerations have a higher variation. This explains why a higher roughness level was obtained when machining below the valley on 6,860 RPM.

The RMS of the full signal was also measured in the time domain, results are shown in Table 10.

	Peak (5535 RPM)	Valley (6860 RPM)
a_x (m/s^2)	0.530	0.914
a_y (m/s^2)	0.747	0.555
a_z (m/s^2)	0.333	0.514

Table 10: RMS time domain for Peak 5,535 RPM and Valley 6,860 RPM.

It is possible to observe that the values are higher for the valley in the x and z directions and higher for the peak in the y direction. Even though the values for the peak in y direction are higher, considering the RMS. The variation between each peak is lower as mentioned before. This should have a higher impact on roughness since the roughness is directly related to the difference between each tooth pass.

The second comparison was made between 13,800 RPM (Valley) and 14,115 RPM (Peak). Figure 41 shows the accelerations in x, y and z for Peak at 14,115 RPM and Figure 42 shows the accelerations in x, y and z for Valley at 13,800 RPM.

Peak – 14,115 RPM

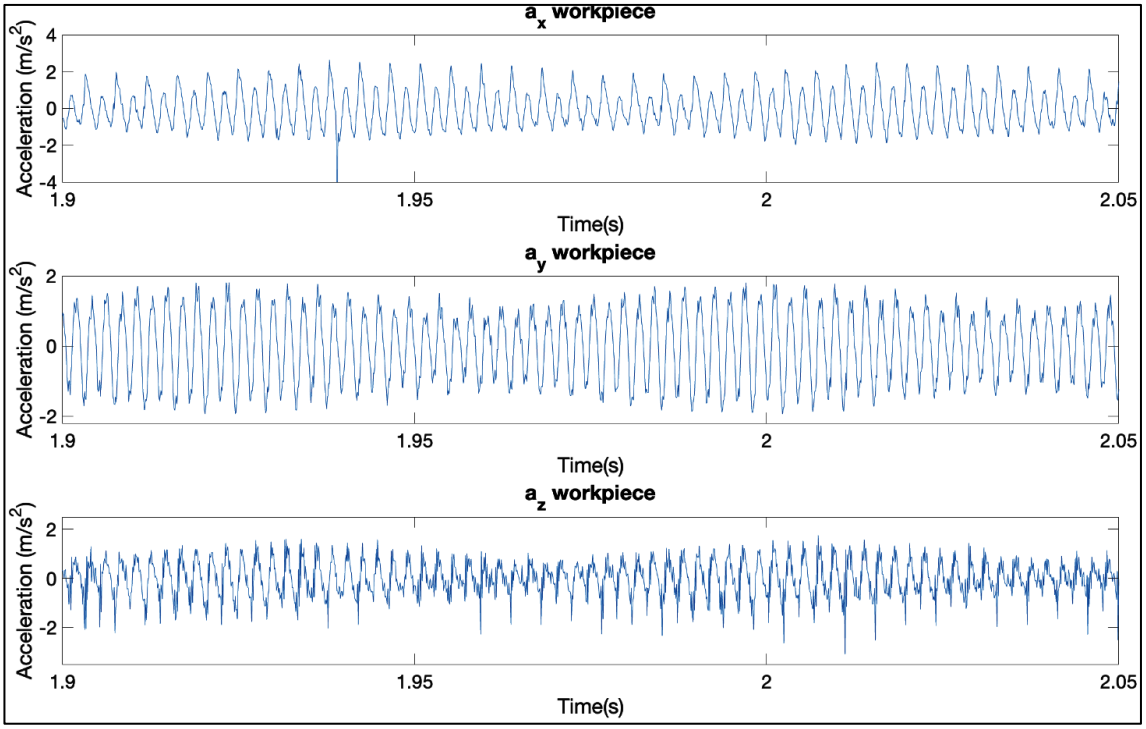

Figure 41: Accelerations in x, y and z for Peak 14,115 RPM.

Valley – 13800 RPM

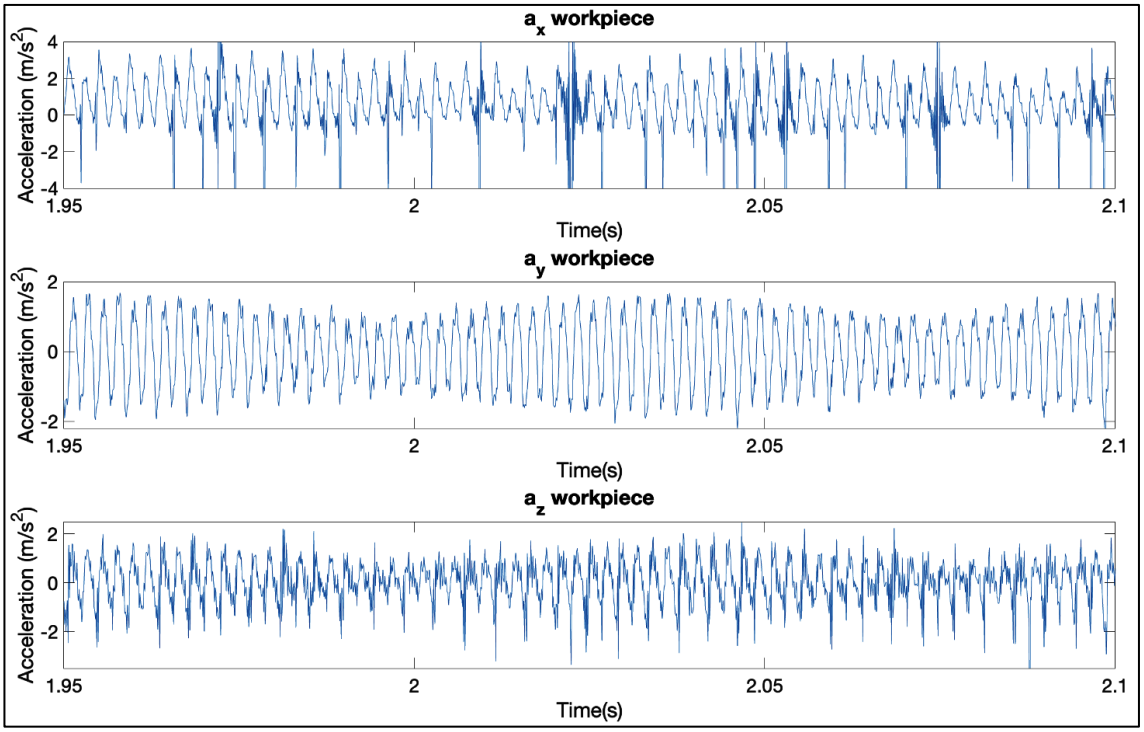

Figure 42: Accelerations in x, y and z for Valley 13,800 RPM.

To observe the acceleration behavior in each pass, a region with reduced sampling time is shown in Figure 43 and Figure 44.

Peak – 14,115 RPM

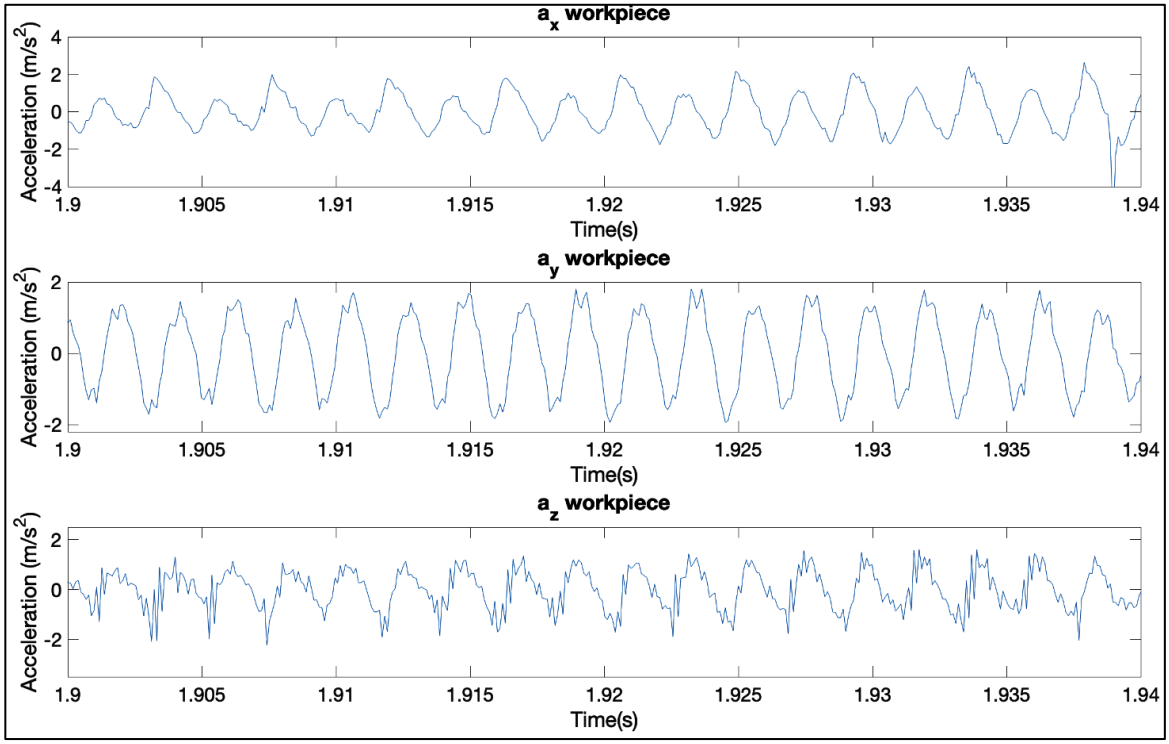

Figure 43: Zoomed accelerations in x, y and z for Peak 14115 RPM.

Valley – 13800 RPM

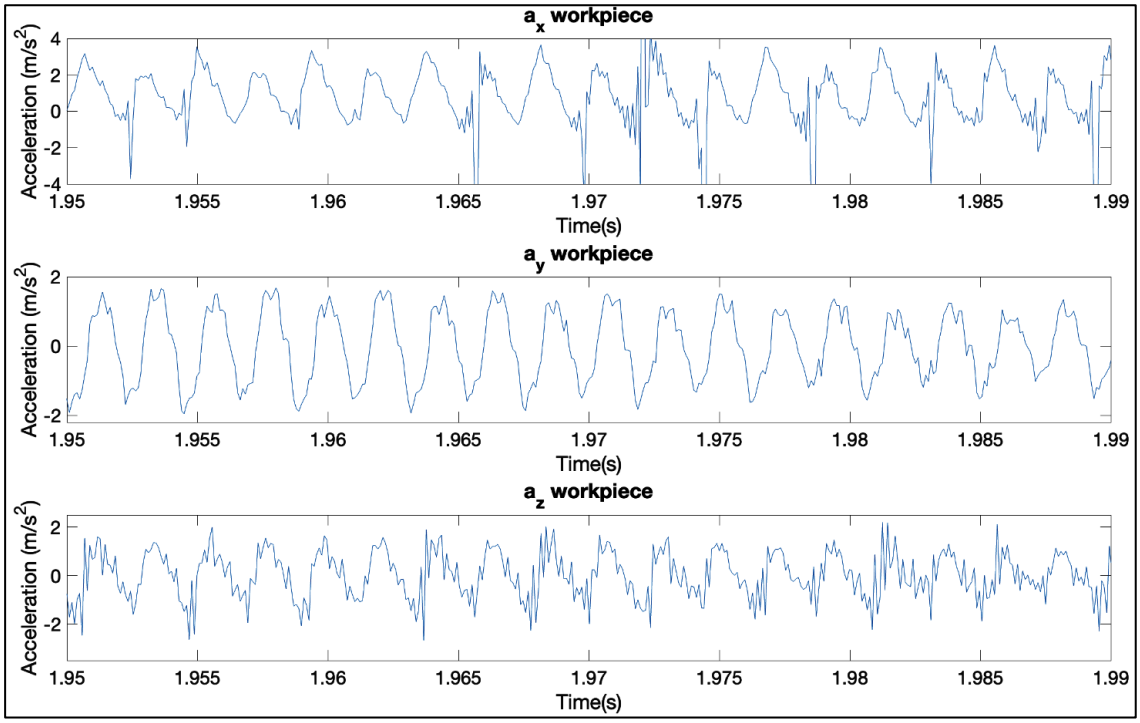

Figure 44: Zoomed accelerations in x, y and z for Valley 13800 RPM.

Comparing both RPMs in Figure 43 and 44 the difference is still noticeable; however, due to the lower difference between roughness values for this region when compared to the other one, the magnitude of the variation is lower. This could be due to the fact the cutting forces are lower for these speeds (higher speeds).

Checking the RMS of the full signal in the time domain in Table 11.

	Peak (14,115 RPM)	Valley (13,800 RPM)
a_x (m/s^2)	1.037	3.493
a_y (m/s^2)	1.006	0.971
a_z (m/s^2)	0.752	1.242

Table 11: RMS time domain for Peak 14,115 RPM and Valley 13,800 RPM.

Again, it is possible to observe that the values are higher for the valley in the x and z directions and high for the peak in the y direction. Even though the values for the peak in y direction are slightly higher considering the RMS. The variation between each peak is lower again. Which explains why the surface roughness was reduced in the peak region.

It is important to mention that even though the variation of roughness is only statistically significant with a confidence below 55% (due to the close mean values). The acceleration analysis confirms the same trend observed in the roughness analysis. In case of the acceleration, the behaviors are different comparing peaks and valleys.

This means that in systems where the cutting conditions are closer to instability, this trend probably will be higher and then the difference in surface roughness will also be higher, which could increase the confidence level of the ANOVA analysis.

CHAPTER 5 – CONCLUSIONS & FUTURE WORKS.

5.1 CONCLUSIONS

- The methodology for roughness identification under b_{lim} was established, which included tool selection, tap test, modal analysis, process parameter selection, surface roughness measurement, data collection and its analysis.
- A methodology has been developed for endmill cutting parameter selection for Aluminum 6066-T6 material where the productivity combined with process integrity is the main objective.
- The effect of the RPM change on surface roughness in stable zone below b_{lim} of SLD is discussed.

The following conclusions are derived from the investigations:

- Even at stable cut regions of the SLD, in this case at 8mm (~42% of b_{lim}), the surface finish is impacted depending on the RPM chosen. Below the peak regions where the stability limits are higher, the roughness tends to be lower. In valley regions, where the stability limits are lower, the roughness tends to be higher.
- The roughness analysis is confirmed by measuring the acceleration of the workpiece. Below valley regions, the accelerations presented a high vibration levels, with higher variation between each tooth pass.

- There is an opportunity to achieve a better surface finish for higher quality products with reduced tool and machine wear by tuning the spindle speed based on system dynamics, even when working at stable regions below b_{lim}.

5.2. FUTURE WORKS

In future research, there are two aspects that could be further studied. The first one is to consider the influence of using a higher stable depth of cut on surface roughness to increase the statistical significance of the results, and the second is the influence of the tool extension from the holder for obtaining more accurate data to increase the confidence levels of the proposed approach.

In conditions closer to instability the trends observed in this research should be intensified. A more conservative approach was used for this work in order to understand that, even when very stable conditions are used, the RPM chosen is important to obtain improved surface roughness which equates to conditions with less tool and machine damage.

In addition, the recommendation is to increase the workpiece length and to perform a greater number of tests. This should increase the number of points and achieve results with higher confidence levels.

There are many factors that must be considered due to the complexity of machining in relationship to making cutting parameter

suggestions. It will be important to see how some of the parameters like speed, feed or depth of cut and tool helix or index geometry can be combined into one framework.

REFERENCES

[1] M. C. (Milton C. Shaw, Metal cutting principles, 2nd ed. in Oxford series on advanced manufacturing ; 5. New York ; Oxford University Press, 2005.

[2] D. A. Stephenson and J. S. Agapiou, Metal Cutting Theory and Practice, 3rd ed. Baton Rouge: CRC Press, 2016. doi: 10.1201/9781315373119.

[3] M. Gomez, A. Honeycutt, and T. Schmitz, “Hybrid manufactured dynamometer for cutting force measurement,” Manuf Lett, vol. 29, pp. 65–69, Aug. 2021, doi: 10.1016/J.MFGLET.2021.06.005.

[4] E. M. (Edward M. Trent and P. K. Wrignt, Metal cutting, 4th ed. San Diego: Butterworth-Heinemann, 2000.

[5] W. Grzesik, Advanced machining processes of metallic materials : theory, modelling, and applications, Second edition. Amsterdam: Elsevier, 2017.

[6] T. R. Soren, R. Kumar, I. Panigrahi, A. K. Sahoo, A. Panda, and R. K. Das, “Machinability behavior of Aluminium Alloys: A Brief Study,” Mater Today Proc, vol. 18, pp. 5069–5075, Jan. 2019, doi: 10.1016/J.MATPR.2019.07.502.

[7] Mdoctor. (n.d.). Machinability of aluminum., “https://www.machiningdoctor.com/machinability/aluminum/.”

[8] E. Karakoç and O. Çakır, “Examination of surface roughness values of 6061-T6 aluminum material after machining and after anodizing process,” Mater Today Proc, vol. 80, pp. 32–39, Jan. 2023, doi: 10.1016/J.MATPR.2022.10.058.

[9] T. Insperger, B. P. Mann, G. Stépán, and P. V. Bayly, “Stability of up-milling and down-milling, part 1: alternative analytical methods,” Int J Mach Tools Manuf, vol. 43, no. 1, pp. 25–34, Jan. 2003, doi: 10.1016/S0890-6955(02)00159-1.

[10] J. Chen, Q. Fang, and P. Li, “Effect of grinding wheel spindle vibration on surface roughness and subsurface damage in brittle material grinding,” Int J Mach Tools Manuf, vol. 91, pp. 12–23, Apr. 2015, doi: 10.1016/J.IJMACHTOOLS.2015.01.003.

[11] J. Eto, T. Hayasaka, and E. Shamoto, “Proposal of novel chatter-free milling strategy utilizing extraordinarily numerous flute endmill and high-

speed high-power machine tool," Precis Eng, vol. 80, pp. 95–103, Mar. 2023, doi: 10.1016/J.PRECISIONENG.2022.11.007.

[12] Y. Altintas, Manufacturing automation : metal cutting mechanics, machine tool vibrations, and CNC design, 2nd ed. Cambridge: Cambridge University Press, 2012.

[13] J. Slavic-Ek, "THE EFFECT OF IRREGULAR TOOTH PITCH ON STABILITY OF MILLING," 1965.

[14] K. Shirase, M. Sano, M. Hirao, and T. Yasui, "Analysis and suppression of chatter vibration in end milling operation (1st report) - Analysis of chatter vibration for irregular tooth pitch end mill using time domain cutting simulation," Seimitsu Kogaku Kaishi/Journal of the Japan Society for Precision Engineering, vol. 65, no. 3, pp. 465–469, 1999.

[15] N. Suzuki, R. Ishiguro, and T. Kojima, "Design of irregular pitch end mills to attain robust suppression of regenerative chatter," CIRP Annals, vol. 65, no. 1, pp. 129–132, Jan. 2016, doi: 10.1016/J.CIRP.2016.04.041.

[16] T. Hayasaka, A. Ito, and E. Shamoto, "Generalized design method of highly-varied-helix end mills for suppression of regenerative chatter in peripheral milling," Precis Eng, vol. 48, pp. 45–59, Apr. 2017, doi: 10.1016/J.PRECISIONENG.2016.11.004.

[17] F. Tehranizadeh, K. Rahimzadeh Berenji, and E. Budak, "Dynamics and chatter stability of crest-cut end mills," Int J Mach Tools Manuf, vol. 171, p. 103813, Dec. 2021, doi: 10.1016/j.ijmachtools.2021.103813.

[18] J. J. Junz Wang and C. S. Yang, "Angle and frequency domain force models for a roughing end mill with a sinusoidal edge profile," Int J Mach Tools Manuf, vol. 43, no. 14, pp. 1509–1520, Nov. 2003, doi: 10.1016/S0890-6955(03)00163-9.

[19] P. Bari, Z. M. Kilic, M. Law, and P. Wahi, "Rapid stability analysis of serrated end mills using graphical-frequency domain methods," Int J Mach Tools Manuf, vol. 171, p. 103805, Dec. 2021, doi: 10.1016/J.IJMACHTOOLS.2021.103805.

[20] M. Imad, "Effect of cutting tool microgeometry when milling hardened steels, a finite element simulation and surface integrity analysis," Jan. 2021, Accessed: Aug. 22, 2022. [Online]. Available: https://ir.library.ontariotechu.ca/handle/10155/1276

[21] Z. Dadić, “(PDF) Tribological principles and measures to reduce cutting tools wear.” Accessed: Dec. 05, 2023. [Online]. Available: https://www.researchgate.net/publication/277202973_Tribological_principles_and_measures_to_reduce_cutting_tools_wear

[22] “Troubleshooting Turning | Tech Tips – Kennametal.” Accessed: Dec. 06, 2023. [Online]. Available: https://www.kennametal.com/ca/en/resources/technical-tips/technical-tips--turning/troubleshooting-turning.html

[23] “How to Avoid 4 Major Types of Tool Wear - In The Loupe.” Accessed: Dec. 06, 2023. [Online]. Available: https://www.harveyperformance.com/in-the-loupe/avoiding-tool-wear/

[24] I. A. Daniyan, I. Tlhabadira, K. Mpofu, and A. O. Adeodu, “Process design and optimization for the milling operation of aluminum alloy (AA6063 T6),” Mater Today Proc, vol. 38, pp. 536–543, Jan. 2021, doi: 10.1016/J.MATPR.2020.02.396.

[25] F. Momeni and J. Ni, “Quality Can Improve as Productivity Increases: Machining as Proof,” Procedia Manuf, vol. 53, pp. 299–309, Jan. 2021, doi: 10.1016/J.PROMFG.2021.06.033.

[26] J. Munoa et al., “Chatter suppression techniques in metal cutting,” CIRP Annals, vol. 65, no. 2, pp. 785–808, Jan. 2016, doi: 10.1016/J.CIRP.2016.06.004.

[27] I. A. Daniyan, I. Tlhabadira, O. O. Daramola, and K. Mpofu, “Design and Optimization of Machining Parameters for Effective AISI P20 Removal Rate during Milling Operation,” Procedia CIRP, vol. 84, pp. 861–867, Jan. 2019, doi: 10.1016/J.PROCIR.2019.04.301.

[28] S. Li, J. Sui, F. Ding, S. Wu, W. Chen, and C. Wang, “Optimization of Milling Aluminum Alloy 6061-T6 using Modified Johnson-Cook Model,” Simul Model Pract Theory, vol. 111, p. 102330, Sep. 2021, doi: 10.1016/J.SIMPAT.2021.102330.

[29] A. Savilov, A. Pyatykh, and A. Nikitenko, “Axial contact points method for improving end-milling productivity,” Mater Today Proc, vol. 38, pp. 1505–1507, Jan. 2021, doi: 10.1016/J.MATPR.2020.08.138.

[30] J. P. Davim, Surface Integrity in Machining, 1. Aufl. London: Springer Verlag London Limited, 2010. doi: 10.1007/978-1-84882-874-2.

[31] N. Geier and C. Pereszlai, “Analysis of Characteristics of Surface Roughness of Machined CFRP Composites,” Periodica Polytechnica Mechanical Engineering, vol. 64, no. 1, pp. 67–80, 2020, doi: 10.3311/PPME.14436.

[32] Z. Yao, J. Shen, M. Wu, D. Zhang, and M. Luo, “Position-dependent milling process monitoring and surface roughness prediction for complex thin-walled blade component,” Mech Syst Signal Process, vol. 198, p. 110439, Sep. 2023, doi: 10.1016/J.YMSSP.2023.110439.

[33] R. Abebe and M. Gopal, “Exploring the effects of vibration on surface roughness during CNC face milling on aluminum 6061-T6 using sound chatter,” Mater Today Proc, vol. 90, pp. 43–49, Jan. 2023, doi: 10.1016/J.MATPR.2023.04.332.

[34] J. P. Davim, Surface Integrity in Machining, 1st ed. 2010. London: Springer London, 2010. doi: 10.1007/978-1-84882-874-2.

[35] Y. Altintas, G. Stepan, D. Merdol, and Z. Dombovari, “Chatter stability of milling in frequency and discrete time domain,” CIRP J Manuf Sci Technol, vol. 1, no. 1, pp. 35–44, Jan. 2008, doi: 10.1016/J.CIRPJ.2008.06.003.

[36] G. Corson, C. Tyler, J. Dvorak, and T. Schmitz, “Minimum cost, stability constrained preform optimization for hybrid manufacturing,” Manuf Lett, vol. 39, pp. 1–5, Jan. 2024, doi: 10.1016/J.MFGLET.2023.10.004.

[37] C. T. Tyler, J. Troutman, and T. L. Schmitz, “Radial depth of cut stability lobe diagrams with process damping effects,” Precis Eng, vol. 40, pp. 318–324, Apr. 2015, doi: 10.1016/J.PRECISIONENG.2014.11.004.

[38] T. L. Schmitz and K. S. Smith, Machining Dynamics, 2nd ed. Cham: Springer International Publishing AG, 2018. doi: 10.1007/978-3-319-93707-6.

[39] S. S. Rao, Mechanical vibrations, 4th ed. Upper Saddle River, N.J: Pearson/Prentice Hall, 2004.

[40] Y. Y. Ren, M. Wan, W. H. Zhang, and Y. Yang, “A review on methods for obtaining dynamical property parameters of machining processes,” Mech Syst Signal Process, vol. 194, p. 110280, Jul. 2023, doi: 10.1016/J.YMSSP.2023.110280.

[41] M. Postel, B. Bugdayci, F. Kuster, and K. Wegener, “Neural network supported inverse parameter identification for stability predictions in

milling," CIRP J Manuf Sci Technol, vol. 29, pp. 71–87, May 2020, doi: 10.1016/J.CIRPJ.2020.02.004.

[42] M. G. T. P. J. M. G Aguirre, "Self-tuning semi-active tuned-mass damper for machine tool chatter suppression." Accessed: Nov. 28, 2023. [Online]. Available: https://scholar.google.es/citations?view_op=view_citation&hl=en&user=MOwjZBQAAAAJ&citation_for_view=MOwjZBQAAAAJ:zYLM7Y9cAGgC

[43] E. B. Kivanc and E. Budak, "Structural modeling of end mills for form error and stability analysis," Int J Mach Tools Manuf, vol. 44, no. 11, pp. 1151–1161, Sep. 2004, doi: 10.1016/J.IJMACHTOOLS.2004.04.002.

[44] Y. Yang, W. Dai, and Q. Liu, "Design and implementation of two-degree-of-freedom tuned mass damper in milling vibration mitigation," J Sound Vib, vol. 335, pp. 78–88, Jan. 2015, doi: 10.1016/J.JSV.2014.09.032.

[45] G. Quintana and J. Ciurana, "Chatter in machining processes: A review," Int J Mach Tools Manuf, vol. 51, no. 5, pp. 363–376, May 2011, doi: 10.1016/J.IJMACHTOOLS.2011.01.001.

[46] R. Rusinek, P. Lajmert, K. Krzysztof, B. Kruszynski, and J. Warminski, "Chatter identification methods on the basis of time series measured during titanium superalloy milling," Int J Mech Sci, vol. 99, pp. 196–207, Aug. 2015, doi: 10.1016/J.IJMECSCI.2015.05.013.

[47] I. Del Sol, A. Rivero, L. N. L. de Lacalle, and A. J. Gamez, "Thin-Wall Machining of Light Alloys: A Review of Models and Industrial Approaches," Materials 2019, Vol. 12, Page 2012, vol. 12, no. 12, p. 2012, Jun. 2019, doi: 10.3390/MA12122012.

[48] S. Tobias, W. F.-T. engineer, and undefined 1958, "Theory of regenerative machine tool chatter," vibraction.frSA Tobias, W FishwickThe engineer, 1958•vibraction.fr, Accessed: Nov. 10, 2023. [Online]. Available: http://www.vibraction.fr/images/stories/Documents/1erePresentationLobesTobias.pdf

[49] Y. Y. Ren, M. Wan, W. H. Zhang, and Y. Yang, "A review on methods for obtaining dynamical property parameters of machining processes," Mech Syst Signal Process, vol. 194, p. 110280, Jul. 2023, doi: 10.1016/J.YMSSP.2023.110280.

[50] D. Li, H. Cao, and X. Chen, "Fuzzy control of milling chatter with piezoelectric actuators embedded to the tool holder," Mech Syst Signal

Process, vol. 148, p. 107190, Feb. 2021, doi: 10.1016/J.YMSSP.2020.107190.

[51] B. Tang, H. Akbari, M. Pouya, and P. V. Pashaki, “Application of piezoelectric patches for chatter suppression in machining processes,” Measurement, vol. 138, pp. 225–231, May 2019, doi: 10.1016/J.MEASUREMENT.2019.02.003.

[52] E. Budak and Y. Altintaş, “Analytical Prediction of Chatter Stability in Milling—Part I: General Formulation,” J Dyn Syst Meas Control, vol. 120, no. 1, pp. 22–30, 1998, doi: 10.1115/1.2801317.

[53] T. Schmitz, J. Nazario, T. No, M. Gomez, and G. Corson, “Time-domain simulation and testing for dynamic force and stability prediction in milling: Collaboration with feed rate scheduling software,” IFAC-PapersOnLine, vol. 55, no. 36, pp. 103–108, Jan. 2022, doi: 10.1016/J.IFACOL.2022.11.341.

[54] E. Karakoç and O. Çakır, “Examination of surface roughness values of 6061-T6 aluminum material after machining and after anodizing process,” Mater Today Proc, vol. 80, pp. 32–39, Jan. 2023, doi: 10.1016/J.MATPR.2022.10.058.

[55] T. L. Schmitz, T. J. Burns, J. C. Ziegert, B. Dutterer, and W. R. Winfough, “Tool Length-Dependent Stability Surfaces,” Machining Science and Technology, vol. 8, no. 3, pp. 377–397, Dec. 2004, doi: 10.1081/MST-200038989.

[56] U. Bravo, O. Altuzarra, L. N. López De Lacalle, J. A. Sánchez, and F. J. Campa, “Stability limits of milling considering the flexibility of the workpiece and the machine,” Int J Mach Tools Manuf, vol. 45, no. 15, pp. 1669–1680, Dec. 2005, doi: 10.1016/J.IJMACHTOOLS.2005.03.004.

[57] C. Cheng, … T. S.-M. S. and, and undefined 2007, “Rotating tool point frequency response prediction using RCSA,” Taylor & FrancisCH Cheng, TL Schmitz, G Scott DuncanMachining Science and Technology, 2007•Taylor & Francis, vol. 11, no. 3, pp. 433–446, Jul. 2016, doi: 10.1080/10910340701539866.

[58] P. Albertelli, M. Goletti, and M. Monno, “A new receptance coupling substructure analysis methodology to improve chatter free cutting conditions prediction,” Int J Mach Tools Manuf, vol. 72, pp. 16–24, Sep. 2013, doi: 10.1016/J.IJMACHTOOLS.2013.05.003.

[59] O. Özşahin and Y. Altintas, “Prediction of frequency response function (FRF) of asymmetric tools from the analytical coupling of spindle and beam

models of holder and tool," Int J Mach Tools Manuf, vol. 92, pp. 31–40, May 2015, doi: 10.1016/J.IJMACHTOOLS.2015.03.001.

[60] F. Montevecchi, N. Grossi, A. Scippa, and G. Campatelli, "Two-points-based receptance coupling method for tool-tip dynamics prediction," Machining Science and Technology, vol. 21, no. 1, pp. 136–156, Jan. 2017, doi: 10.1080/10910344.2016.1260435.

[61] J. Yulei Shanghai Jiao et al., "A robust RCSA-based method for the in situ measurement of rotating tool-tip frequency response functions," asmedigitalcollection.asme.orgY Ji, QZ Bi, L Yu, F Ren, Y WangJournal of Manufacturing Science and Engineering, 2020•asmedigitalcollection.asme.org, 2020, doi: 10.1115/1.4046989.

[62] Y. Ji, H. Dong, L. Yu, F. Ren, Q. Bi, and Y. Wang, "Determining rotating tool-tip FRFs by measuring holder-point FRFs based on a robust frequency-based substructure method," Mech Syst Signal Process, vol. 164, p. 108228, Feb. 2022, doi: 10.1016/J.YMSSP.2021.108228.

[63] V. Gagnol, B. C. Bouzgarrou, P. Ray, and C. Barra, "Model-based chatter stability prediction for high-speed spindles," Int J Mach Tools Manuf, vol. 47, no. 7–8, pp. 1176–1186, Jun. 2007, doi: 10.1016/J.IJMACHTOOLS.2006.09.002.

[64] M. Wan, X. Bin Dang, W. H. Zhang, and Y. Yang, "Chatter suppression in the milling process of the weakly-rigid workpiece through a moving fixture," J Mater Process Technol, vol. 299, p. 117293, Jan. 2022, doi: 10.1016/J.JMATPROTEC.2021.117293.

[65] C. YUE, H. GAO, X. LIU, S. Y. LIANG, and L. WANG, "A review of chatter vibration research in milling," Chinese Journal of Aeronautics, vol. 32, no. 2, pp. 215–242, Feb. 2019, doi: 10.1016/J.CJA.2018.11.007.

[66] "FUNDAMENTALS OF MACHINING Start to Finish Guide," 2013.

[67] G. Quintana and J. Ciurana, "Chatter in machining processes: A review," Int J Mach Tools Manuf, vol. 51, no. 5, pp. 363–376, May 2011, doi: 10.1016/J.IJMACHTOOLS.2011.01.001.

[68] X. Sun et al., "Material properties and machining characteristics under high strain rate in ultra-precision and ultra-high-speed machining process: a review," International journal of advanced manufacturing technology, vol. 120, no. 11–12, pp. 7011–7042, 2022, doi: 10.1007/s00170-022-09111-5.